Hybrid Bidentate Phosphoramidite Ligands in Asymmetric Catalysis

Fabien Boeda[#], Thomas Beneyton and Christophe Crévisy *

Laboratoire Sciences Chimiques de Rennes, associated with CNRS, ENSCR, Avenue du Général Leclerc, 35700 Rennes, France

[#]*Current address: Institute of Chemical Research of Catalonia (ICIQ), Av. Països Catalans, 16, 43007 Tarragona, Spain*

Abstract: Hybrid bidentate phosphoramidite ligands are a recent family of promising phosphorus ligands. The different classes (phosphoramidite-phosphine, phosphoramidite-phosphite, phosphoramidite-phosphinite, phosphoramidite-thioethers, phosphoramidite-amine, phosphoramidite-NHC, phosphoramidite-oxazoline) are presented along with the strategies used to access to these compounds. The main part of the review summarizes the results of the evaluation of these ligands in reactions catalyzed by transition metals/bidentate phosphoramidite ligands, such as hydrogenation, hydroformylation, conjugate addition and Tsuji-Trost reaction.

Keywords: Hybrid bidentate ligands, phosphoramidites, asymmetric catalysis.

1. INTRODUCTION

Since the seminal work by Knowles in 1968, many chiral ligands have been developed to be applied in metal-catalyzed asymmetric reactions [1a]. C_2-Symmetric bisphosphine ligands were first developed [1]. Some unsymmetrical bisphosphine ligands were later studied and they showed a remarkable efficiency (e.g. Josiphos [2]). Nevertheless, many bisphosphine ligands suffer from lengthy and costly synthetic procedures and some are also poorly stable towards air and high temperatures. Hence, the development of new classes of ligands was of great interest, particularly for industrial applications [3]. In this context, since 1996, there has been a growing interest for monodentate phosphoramidite ligands [4]. In such compounds, a diol unit, usually a biphenol, and an amine unit are linked by a phosphorus atom (Scheme **1**). These ligands are readily accessible and present modular and tunable structures. They have been successfully used in many reactions catalyzed by organotransition metal complexes, such as for instance asymmetric hydrogenation [5], allylic substitution [6], hydrosilylation [7], hydrovinylation [8], hydroboration [9], conjugate addition [10]. The development of unsymmetrical ligands that would exhibit both the advantages of monodentate phosphoramidites and the great efficiency of sterically and electronically unsymmetrical bidentate ligands [11] was very attractive. Furthermore, the quest for "perfect" ligands is far from being over; such optimal ligands should 1) not be too much substrate and reaction specific, 2) exhibit high TONs and TOFs, 3) be readily accessible in both enantiomeric forms from cheap starting material, 4) be air- and moisture-stable, 5) allow the access to a high structural variability, 6) be chemoselective with elaborate substrates. In this context, hybrid bidentate phosphoramidite ligands appeared recently. These ligands display two coordination sites, a phosphoramidite moiety along with a second coordination site being for instance a phosphine or a phosphite (Scheme **1**). The purpose of this review is to present two important aspects dealing with these ligands: 1) Their accessibility; the synthetic routes by which they were obtained will be discussed, 2) Their efficiency; especially the enantioselectivity, the catalyst loading and the substrate scope of the reactions to which their metal complexes have been applied.

*Address correspondence to this author at the Laboratoire Sciences Chimiques de Rennes, associated with CNRS, ENSCR, Avenue du Général Leclerc, 35700 Rennes, France; Tel: (33) 2 23 23 80 74; Fax: (33) 2 23 23 81 08; E-mail: christophe.crevisy@ensc-rennes.fr

2. PREPARATION OF HYBRID BIDENTATE PHOSPHORAMIDITE LIGANDS AND EVALUATION IN ASYMMETRIC CATALYSIS

2.1. Phosphoramidite-phosphine ligands

2.1.1. Overview

The first examples of hybrid bidentate phosphoramidite ligands are the phosphoramidite-phosphine QUINAPHOS **L1a-b** which were reported by Leitner in 2000 (Scheme **2**) [12a]. It is worth noting that **L1a-b** bear a BINOL moiety as many mono- and bi-dentate phosphoramidites. Leitner also reported the synthesis of isomers **L1c-d** and analogues **L1e-h** and **L2**, the latter being obtained from a biphenol moiety (Scheme **2**) [12a, 12b]. Since then, many phosphoramidite-phosphine ligands were synthesized; their structures are depicted in Scheme **2**.

As the diol part of these ligands is usually a biphenol-type framework (BINOL, H8-BINOL, biphenol, catechol), the structural difference between them lies essentially in the amino part which often carries the phosphino coordination site. The first class of amine contains cyclic amines as chiral 2-alkyl-1,2-dihydroquinoline found in ligands **L1-2** and also non chiral 3-methylindole found in INDOLPhos **L3a-d** [13]. The second class consists of chiral ferrocene-based diarylphosphino-amines (**L4a-l**, Scheme **2**) [14-17]. The third class is derivatized from benzylamines and arylamines (e.g. anilines) which can be chiral, as in ligands **L5a-d** [18] and **L5e** [19] or not, as in Me-anilaphos **L5f** [20] and ligand **L5g** [21]. Chiral (*R*)-1,2,3,4-tetrahydro-1-naphtylamine found in ligands **5h-i** [22] may also be included in this class. The fourth class contains chiral-pool based diphenylphosphino-amines as in ligand **L6** which derived from phenylalanine [23]. Very recently, Zhang reported a different type of phosphoramidite-phosphine ligands (**L7a-d**) in which the phos-

1570-193X/08 $55.00+.00

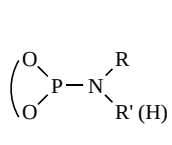

Monodentate phosphoramidite ligand

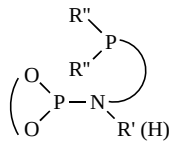

Bidentate phosphoramidite-phosphine ligand

Scheme 1.

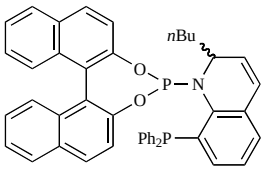

(*Rc*,*Ra*)-Quinaphos **L1a** and (*Sc*,*Ra*)-Quinaphos **L1b**
(*Rc*,*Sa*)-Quinaphos **L1c** and (*Sc*,*Sa*)-Quinaphos **L1d**

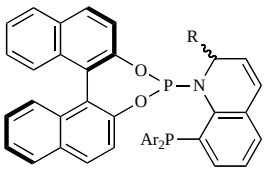

(*Rc*,*Ra*), R = *t*Bu, Ar = Ph **L1e**
(*Sc*,*Ra*), R = *t*Bu, Ar = Ph **L1f**
(*Rc*,*Ra*), R = *n*Bu, Ar =*o*-toluyl-$(CH)_2(CF_2)_6F$ **L1g**
(Sc,*Ra*), R = *n*Bu, Ar =*o*-toluyl-$(CH)_2(CF_2)_6F$ **L1h**

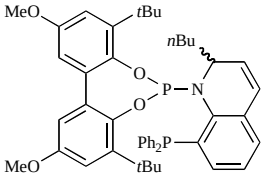

L2

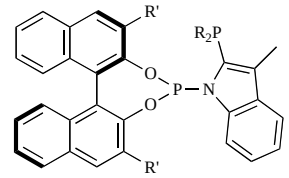

R = Ph, R' = H **L3a**
R = *i*Pr, R' = H **L3b**
R = Ph, R' = $SiMe_3$ **L3c**
R = *i*Pr, R' = Me **L3d**

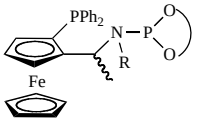

R = Me, Diol = BINOL, (*Sc, Rp, Ra*) **L4b**
R = Me, Diol = BINOL, (*Sc, Rp, Sa*) **L4c**
R = Me, Diol = biphenol, (*Sc, Rp*) **L4d**
R = Me, Diol = catechol, (*Sc, Rp*) **L4e**
R = Me, Diol = H8-BINOL, (*Sc, Rp, Sa*) **L4f**
R = Et, Diol = H8-BINOL, (*Sc, Rp, Sa*) **L4g**
R = H, Diol = H8-BINOL, (*Sc, Rp, Sa*) **L4h**
R = H, Diol = BINOL, (*Sc, Rp, Sa*) **L4i**

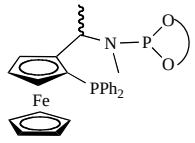

Diol = BINOL, (*Sc, Sp, Ra*) **L4j**
Diol = BINOL, (*Sc, Sp, Sa*) **L4k**
Diol = H8-BINOL, (*Rc, Sp, Sa*) **L4l**

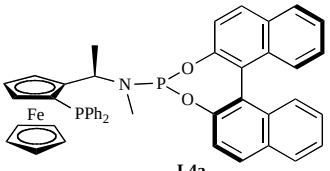

L4a (*Ra*)

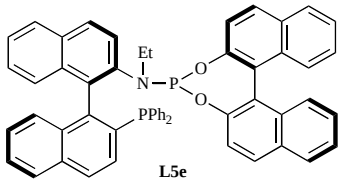

L5e

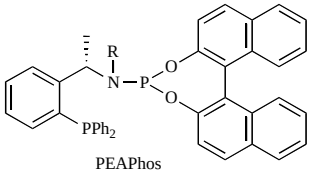

PEAPhos

(*Ra*), R = H **L5a**
(*Sa*), R = H **L5b**
(*Ra*), R = Me **L5c**
(*Sa*), R = Me **L5d**

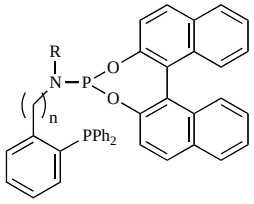

(*Ra*), R = Me, n = 0 **L5f**
(*Sa*), R = CH_2Ph, n = 1 **L5g**

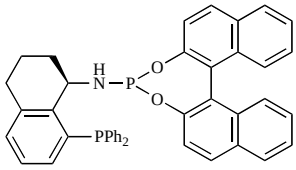

(*Rc*, *Ra*) **L5h**
(*Rc*, *Sa*) **L5i**

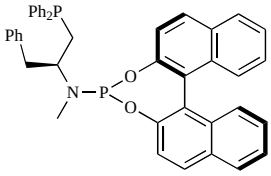

L6

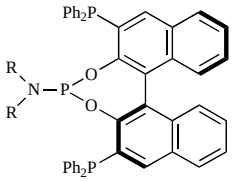

R = Me **L7a**
R = Et **L7b**
R = *i*Pr **L7c**
R, R = -$(CH_2)_5$- **L7d**

Scheme 2.

phine coordination site is located in the BINOL framework instead of being in the amine part of the molecule [24].

2.1.2. Synthesis of Phosphoramidite-Phosphine Ligands

Ligands **L1**-**L6** were obtained using the same strategy: a diarylphosphino-amine was synthesized and then reacted with the diol and PCl_3 in the presence of a base.

Ligands **L1**-**L2** were obtained in a two steps procedure (Scheme **3**) [12, 25]. 8-bromoquinoleine **1** was successively treated with *n*BuLi and Ar_2PCl to give 8-bisarylphosphanyl-quinoleine **2.** Compound **2** was submitted to a nucleophilic addition of an organolithium reagent to give lithium salt **3**. The latter was then added to a chlorophosphite, which was prepared according to classical conditions [26]. A mixture of

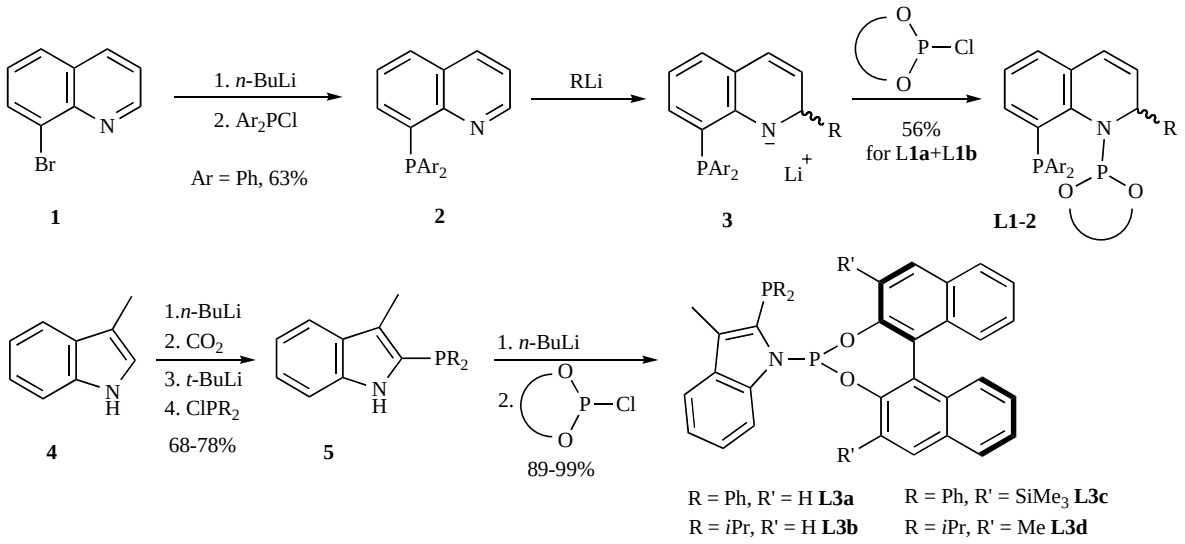

Scheme 3.

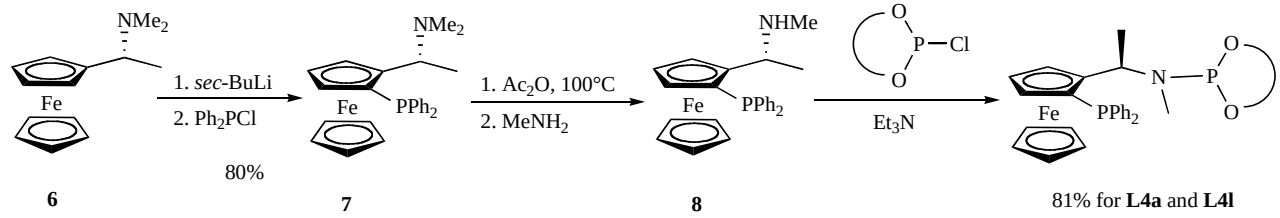

Scheme 4.

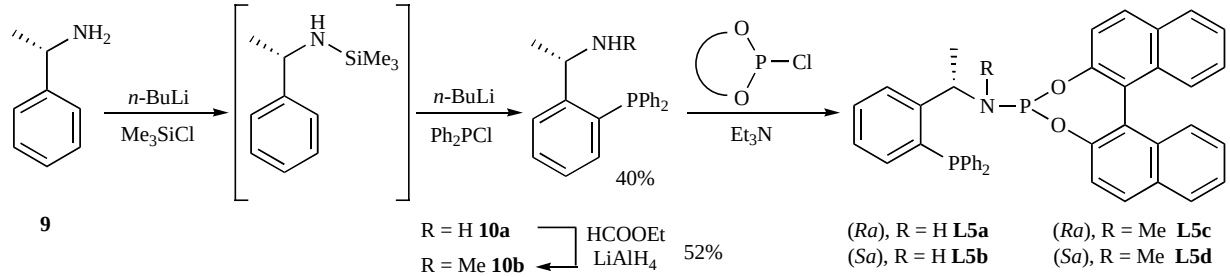

Scheme 5.

diastereoisomers was obtained so that a separation was required. Ligands **L3a-d** were readily prepared in two steps from 3-methylindole **4** [13]. Aminophosphine **5** was first obtained by a directed metalation reaction then converted to the expected ligand following a standard procedure employed for the synthesis of phosphoramidite group (Scheme **3**) [26].

Zheng, Chan and Li reported the synthesis of various ferrocene-based phosphoramidite-phosphine ligands **L4a-l**. Ligands **L4a** and **L4l** were prepared from commercially available *N*,*N*-dimethyl-(*R*)-α-ferrocenylethylamine **6** in a 4 step-procedure as outlined in Scheme **4** [14, 17, 27b]. Amine **6** was treated successively with *sec*-BuLi and Ph_2PCl to give the amino-phosphine **7**. The substitution of the dimethyl amino group by a secondary amine was performed by sequential treatment of **7** with Ac_2O then methylamine. The reaction of the resulting amine **8** with the appropriate chlorophosphite under standard conditions [26] gave the expected ligands.

Isomeric ligands **L4b-k** were prepared from *N*,*N*-dimethyl-(*S*)-α-ferrocenylethylamine following a similar strategy [15, 16, 17, 27], but the preparation of **L4j** and **L4k** was more laborious [15].

Ligands **L5a-d** were synthesized in a 2 or 3 step-procedure as outlined in Scheme **5** [18]. (*S*) Phenylethylamine **9** was sequentially treated by *n*BuLi and TMSCl to give an intermediate which was dilithiated by further addition of *n*BuLi. After subsequent orthophosphination with Ph_2PCl, the resulting diphenylphosphino-amine **10a** could be monomethylated to give secondary amine **10b**. Amines **10a** and **10b** were converted to ligands **L5a-d** according to the

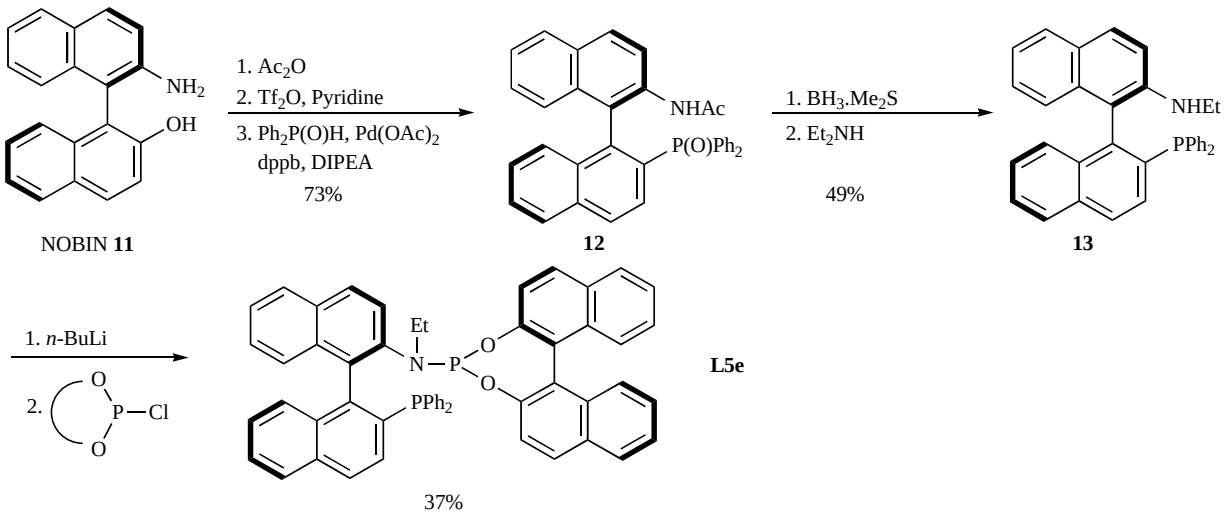

Scheme 6.

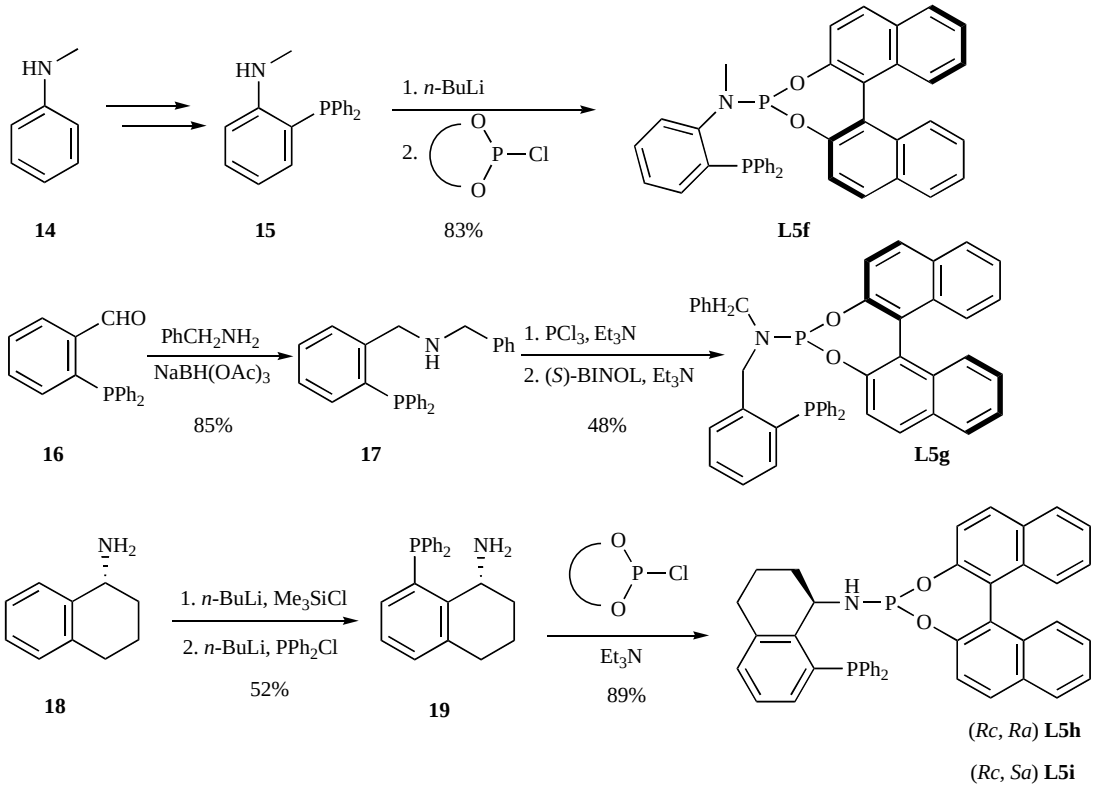

Scheme 7.

classical conditions used for the formation of phosphoramidites [26].

Ligand **L5e** was prepared in a five step-procedure from NOBIN **11** (Scheme **6**) [19]. NOBIN was subsequently *N*-acetylated then *O*-triflated to give a product which was submitted to a Pd–catalyzed phosphonoylation to afford compound **12**. Reduction of both phosphine oxide and acetamide groups afforded amino-phosphine **13** which was deprotonated before being quenched with chlorophosphite to give **L5e** in a rather low yield.

Ligand **L5f** was prepared in one step from 2-diphenylphosphino-*N*-dimethylaniline **15** [20] which in turn can be readily obtained from *N*-methylaniline **14** (Scheme **7**) [28]. Our group prepared ligand **L5g** in a short two-step procedure from *o*-diphenylphosphinobenzaldehyde **16** [21]. Aminophosphine **17** was obtained by a reductive amination on aldehyde **16**. Ligand **L5g** was then synthesized by treatment of **17** with PCl_3 and subsequent reaction of the resulting aminodichlorophosphine with (*S*)-BINOL (Scheme **7**) [26]. Ligands **L5h**-**i** were easily obtained in a two-step procedure from commercially available (*R*)-1,2,3,4-tetrahydro-1-naphtylamine **18** [22]. Position 8 was metalated and the resulting salt was quenched with Ph_2PCl to give aminophosphine **19,** which was converted to expected ligands according to standard procedures (Scheme **7**) [26].

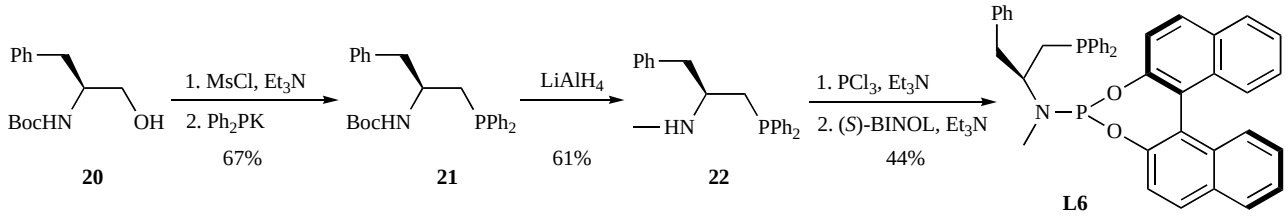

Scheme 8.

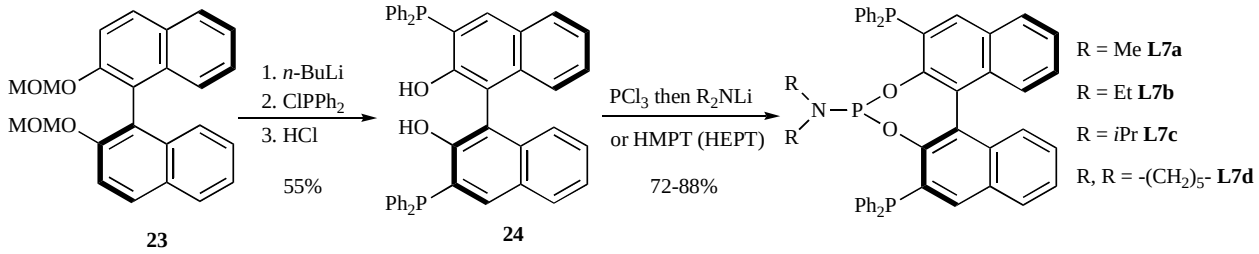

Scheme 9.

Our group reported the preparation of ligand **L6** from commercially available Boc-phenylalaninol **20** (Scheme **8**) [23]. Conversion of the hydroxyl group to a better leaving group followed by a nucleophilic displacement with PPh_2K gave phosphine **21**. The reduction of the Boc group afforded the amine **22**. The latter was converted to **L6** following classical conditions employed for the formation of phosphoramidites [26].

As in ligands **L7** the diphenylphosphino group is carried by the diol part of the molecule, a different strategy had to be employed for their synthesis. *Ortho*-substituted diphenylphosphino BINOL **24** was first synthesized as outlined in scheme **9** [24]. Lithiation of the MOM-protected BINOL **23** followed by treatment with Ph_2PCl and deprotection of the MOM groups gave compound **24**. The latter was converted to the expected ligands following one of the two classical procedures; either generation of the corresponding chlorophosphite was followed by addition of a lithium amide (for **L7c-d**), or the biphenol **24** was heated with HEPT or HMPT (for **L7a-b**).

2.1.3. Evaluation of Phosphoramidite-Phosphine Ligands in Asymmetric Catalysis

Ligands **L1**-**L5** and **L7** were almost all evaluated towards organotransition-metal catalyzed asymmetric hydrogenation of C-C double bonds. QUINAPHOS **L1a**-**L1b**, ligands **L3a-d** and **L5e** were examined in asymmetric hydroformylation. QUINAPHOS **L1a-L1b** were also applied to the Ru-catalyzed asymmetric hydrogenation of ketones, while **L6** was examined in Cu-catalyzed conjugated addition to enones.

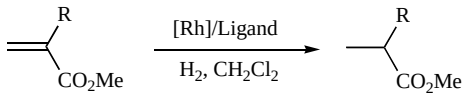

Scheme 10.

2.1.3.1. Hydrogenation of Carbon-Carbon Double Bonds

Diastereoisomeric **L1a** and **L1b** were evaluated towards Rh-catalyzed hydrogenation of dimethyl itaconate **S1a** and methyl-2-acetamidoacrylate **S2** (Scheme **10**, Table **1**) [12a]. The reactions were conducted at room temperature, in the presence of 0.1 mol % of catalyst and under high pression of hydrogen. The best enantioselectivity (98.8% ee) was obtained using 2.2 molar equivalents of the (*Rc*, *Ra*) isomer **L1a** in the hydrogenation of **S1a**. Under the same conditions, a poor result (12.4% ee) was obtained in the hydrogenation

Table 1. Hydrogenation of dimethyl itaconate S1a and methyl 2-acetamidoacrylate S2 catalyzed by Rh-QUINAPHOS complexes[a]

Entry	Ligand	Substrate	Ligand/Rh	Conv. (%)	e.e. (%)
1	**L1b**	**S1a**	1.1	> 99	64.2 (*R*)
2	**L1b**	**S1a**	2.2	> 99	78.8 (*R*)
3	**L1a**	**S1a**	1.1	> 99	95.6 (*R*)
4	**L1a**	**S1a**	2.2	> 99	98.8 (*R*)
5	**L1a**	**S2**	2.2	8.0	12.4 (*S*)
6	**L1a**	**S2**	1.0[b]	> 99	97.8 (*S*)

[a] Hydrogenation was performed at room temperature under an H_2 pressure of 30 bars for 24h and the catalyst was made in situ from 0,1 mol % of $[Rh(cod)_2]BF_4$.

[b] Isolated complex [(**L1a**)Rh(cod)]BF_4 **25** was used as the catalyst.

Table 2. Rh/L3a-d catalyzed hydrogenation of S1a and S2[a, b]

Entry	Ligand	Substrate	e.e. (%)
1	**L3a**[c]	**S1a**	73 (*S*)
2	**L3b**	**S1a**	98 (*S*)
3	**L3c**[d]	**S1a**	12 (*S*)
4	**L3d**	**S1a**	92 (*S*)
5	**L3a**[c]	**S2**	13 (*S*)
6	**L3b**	**S2**	86 (*R*)
7	**L3c**[d]	**S2**	36 (*R*)
8	**L3d**	**S2**	97 (*R*)

[a] Full conversion was obtained for all reactions.
[b] The reactions were conducted for 16h at 25°C under an H_2 pressure of 10 bars. The catalyst was made in situ from 1.0 mol % of $[Rh(nbd)_2]BF_4$.
[c] A 1:4 mixture of [Rh(**L3a**)(nbd)]BF_4 and [Rh(**L3a**)$_2$]BF_4 was formed by mixing the ligand with 1 eq. of $[Rh(nbd)_2]BF_4$.
[d] The isolated complex [Rh(**L3c**)(cod)]BF_4 was used.

of **S2**. However, a high enantioselectivity (97.8%) was achieved when the isolated complex [(**L1a**)Rh(cod)]BF_4 **25** was used (entry 6). The hydrogenation of dimethyl itaconate **S1a** was also accomplished with a high activity, as a TOF of over 35000 h^{-1} was estimated.

Reek recently described his findings about the use of INDOLPhos ligands **L3a-d** in the rhodium-catalyzed hydrogenation of itaconate **S1a** and methyl-2-acetamidoacrylate **S2** (Scheme **10**, Table **2**) [13]. The reactions were carried out with 1.0 mol % of the catalyst under 10 bars of H_2. The presence of the bulky diisopropylphosphine group proved to be important to obtain good enantioselectivities in the hydrogenation of both substrates (entries 2, 4, 6, 8). Moreover, the enantioselectivity was further increased when the ligand **L3d**, possessing an *ortho*-methyl-substituted BINOL group, was used in the hydrogenation of **S2** (entry 8).

Ferrocene-based ligands **L4a**, **L4c**, **L4f-h** and **L4l** were tested in the rhodium-catalyzed hydrogenation of α-dehydroamino acid derivatives **S3a**-**S3l** (Scheme **11**, Table **3**) [14, 15, 17]. Very high enantioselectivities (99-99.9% ee) were obtained with almost all substrates and ligands. However, ligand **L4l** seems to be the unmatched isomer for the H8-BINOL-derived ligands as a moderate enantioselectivity was observed when it was used (entry 12). The enantioselectivities did not depend upon the electronic properties of the aryl group (entries 13-18) except for ligand **L4a** where the presence of the electron donating methyl group in **S3c** decreased the enantioselectivity (97.4% entry 3). Ligand **L4c** and **L4f** remained very efficient even when the catalyst loading was decreased from 1.0 to 0.1 mol% (entries 7 and 9). It is noteworthy that the Rh/**L4c**-catalyzed hydrogenation of **S3a** gave a better result in term of enantioselectivity when it proceeded with of 2.2 equiv. of ligand per rhodium and in the presence of a small amount of air or moisture (entry 7). The authors also observed that the enantioselectivity of the reaction was solvent dependent with some ligands (**L4a)** and not with others (**L4c** and **L4f)**. The Rh/**L4f**-catalyzed hydrogenation of **S3a** was also studied at lower H_2 pressure (1 bar)

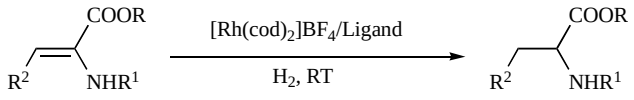

S3a : R = Me, R^1 = CH_3CO, R^2 = Ph	**P3a**
S3b : R = Me, R^1 = CH_3CO, R^2 = *p*-NO_2-Ph	**P3b**
S3c : R = Me, R^1 = CH_3CO, R^2 = *p*-Me-Ph	**P3c**
S3d : R = Me, R^1 = PhCO, R^2 = *p*-F-Ph	**P3d**
S3e : R = Me, R^1 = CH_3CO, R^2 = *p*-Br-Ph	**P3e**
S3f : R = Me, R^1 = PhCO, R^2 = *p*-Cl-Ph	**P3f**
S3g : R = Et, R^1 = CH_3CO, R^2 = Ph	**P3g**
S3h : R = Me, R^1 = CH_3CO, R^2 = *o*-Cl-Ph	**P3h**
S3i : R = Me, R^1 = CH_3CO, R^2 = *p*-Cl-Ph	**P3i**
S3j : R = Et, R^1 = CH_3CO, R^2 = *p*-Cl-Ph	**P3j**
S3k : R = Me, R^1 = CH_3CO, R^2 = *o*-OMe-Ph	**P3k**
S3l : R = Me, R^1 = CH_3CO, R^2 = *p*-OMe-Ph	**P3l**
S3m : R = Me, R^1 = CH_3CO, R^2 = *p*-F-Ph	**P3m**
S3n : R = Me, R^1 = CH_3CO, R^2 = *m*-Br-Ph	**P3n**
S3o : R = Me, R^1 = CH_3CO, R^2 = *p*-CF_3-Ph	**P3o**
S3p : R = Me, R^1 = CH_3CO, R^2 = thiophenyl	**P3p**
S3q : R = Me, R^1 = CH_3CO, R^2 = *n*-Pr	**P3q**
S3r : R = Me, R^1 = CH_3CO, R^2 = $MeOCH_2$	**P3r**
S2 : R = Me, R^1 = CH_3CO, R^2 = H	**P2**

Scheme 11.

in MeOH and no significant drop of the ee value was observed under these conditions. Finally, no clear-cut difference in the enantioselectivity was noted between BINOL-based ligand **L4c** and the corresponding H8-BINOL-derived ligand **L4f** (entries 7, 9).

Ferrocene-based ligands **L4a-h** and **L4j-l** were tested in the rhodium-catalyzed hydrogenation of enamides **S4a**-**S4h** (Scheme **12**, Table **4**) [14, 15, 17]. Among all the ligands tested, **L4c** and **L4j** exhibited the best enantioselectivities in the hydrogenation of compound **S4a** (entries 1-11). Very high ee's were also obtained with substrates **S4b-e** (entries 12-15). It is noteworthy that H8-BINOL-based ligands gave slightly lower enantioselectivities than the corresponding BINOL-based ligands in the hydrogenation of **S4a** (entries 3 and 6). Similar results were obtained with substrates **S4c**-**S4e** [17]. While (*Sc*,*Rp*,*Sa*)-**L4c** and (*Sc*,*Sp*,*Ra*)-**L4j** gave hydrogenated products **P4a** of opposite configurations (entries 3 and 9), (*Sc*,*Rp*,*Sa*)-**L4c** and (*Sc*,*Sp*,*Sa*)-**L4k** gave the same enantiomer (entries 3 and 10). Moreover, biphenol- and catechol-based ligands **L4d** and **L4e** afforded a product with a lower ee (entries 4 and 5). Ultimately, it appears that the BINOL moiety plays a critical role in the stereochemical outcome.

The catalytic performance of ferrocene-based ligands **L4** was also tested in the Rh-catalyzed hydrogenation of dimethyl itaconate **S1a** (Scheme **10**, Table **5**) [15, 17]. Ligands **L4c**, **L4f** and **L4h** afforded the product with the highest enantioselectivity (99.9% ee, entries 1-3) while unmatched

Table 3. Rh/ferrocene-based ligands L4a-L4f catalyzed hydrogenation of α-dehydroamino acid derivatives S3

Entry	Ligand	Substrate	Rh/L (mol %)	Solvent, Pressure (bar)	Time (h) [a]	e.e. (%)
1	**L4a**	**S3a**	1/1.1	THF, 20	-	99 (*S*)
2	**L4a**	**S3b**	1/1.1	THF, 20	-	99.6 (*S*)
3	**L4a**	**S3c**	1/1.1	THF, 20	-	97.4 (*S*)
4	**L4a**	**S3d**	1/1.1	THF, 20	-	99 (*S*)
5	**L4a**	**S3e**	1/1.1	THF, 20	-	99 (*S*)
6	**L4a**	**S3f**	1/1.1	THF, 20	-	99 (*S*)
7	**L4c**	**S3a**	0.1/0.22[b]	CH_2Cl_2, 10	1	99.9 (*R*)
8	**L4f**	**S3a**	1/1.1	CH_2Cl_2, 10	24	99.9 (*R*)
9	**L4f**	**S3a**	0.1/0.11	CH_2Cl_2, 10	24	99.8 (*R*)
10	**L4g**	**S3a**	1/1.1	CH_2Cl_2, 10	24	99.9 (*R*)
11	**L4h**	**S3a**	1/1.1	CH_2Cl_2, 10	24	99.8 (*R*)
12	**L4l**	**S3a**	1/1.1	CH_2Cl_2, 10	24	50.0 (*R*)
13	**L4f**	**S3g**	1/1.1	CH_2Cl_2, 10	24	99.7 (*R*)
14	**L4f**	**S3h**	1/1.1	CH_2Cl_2, 10	24	99.8 (*R*)
15	**L4f**	**S3i**	1/1.1	CH_2Cl_2, 10	24	99.7 (*R*)
16	**L4f**	**S3j**	1/1.1	CH_2Cl_2, 10	24	99.5 (*R*)
17	**L4f**	**S3k**	1/1.1	CH_2Cl_2, 10	24	99.8 (*R*)
18	**L4f**	**S3l**	1/1.1	CH_2Cl_2, 10	24	99.7 (*R*)

[a] Complete conversion was obtained in all reactions. [b] The reaction was carried out under unprotected conditions. A 99.0% ee value was obtained when the reaction was performed in a glove box with dried, degassed solvents and a purged autoclave.

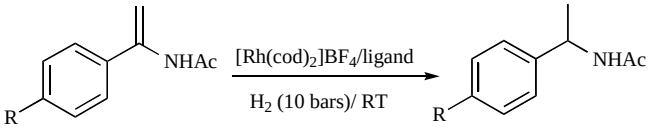

S4a : R = H — **P4a**
S4b : R = F — **P4b**
S4c : R = Cl — **P4c**
S4d : R = Br — **P4d**
S4e : R = CF_3 — **P4e**
S4f : R = Me — **P4f**
S4g : R = OMe — **P4g**
S4h : R = *m*-OMe — **P4h**

Scheme 12.

ligand **L4l** gave a poor ee value (entry 5). It must be underlined that BINOL- **L4c** and the corresponding H8-BINOL-**L4f** based ligands led to the same ee values. On the other hand Rh/**L4c** complex appeared to be far more active than Rh/**L4f**, as the reaction was finished with the former after a short period of time although a lower catalyst loading was used (entries 1 and 2). Moreover, when a low loading of Rh/**L4c** catalyst (0.01 mol %) was used, the enantioselectivity was only slightly diminished (99.1% ee) [15]. It is interesting to note that similar ee values were obtained in various solvents or under an H_2 pressure of 1 bar.

Zheng observed unsatisfactory results in the Rh/**L4c** catalyzed hydrogenation of β-aryl-β-(acylamino)acrylate (*Z*)-**S5a** (Scheme **13**, Table **6**, entry 1). It had already been noted that Bophoz-H was a better ligand than Bophoz-Me in the Rh-catalyzed hydrogenation reaction. As a consequence, Zheng anticipated that an analogue of **L4c** where the N-Me group would have been replaced by a N-H group could allow for higher enantioselectivities. As expected, an excellent ee value was obtained with **L4i** (>99% ee, entry 2) [16]. Various β-aryl-β-(acylamino)acrylates were tested in the Rh-**L4i** catalyzed reaction and no influence of the electronic properties of the aryl group of the substrates could be noticed, but higher enantioselectivities (98->99% ee) were obtained with ethylacrylates **S5a, S5b, S5d, S5f** compared to those obtained with methylacrylates (97-98% ee) [16]. A minor deterioration in the ee occurred when the catalyst loading was decreased from 1.0 mol% to 0.1 mol % (entries 2 and 3). The catalytic system based on **L4i** was next applied to β-alkyl-β-(acylamino)acrylates **S5j**-**S5n**. While (*E*)- β-alkyl-β-(acylamino)acrylates afforded hydrogenated products with enantiomeric excess (97-99% ee) close to those obtained with β-aryl-β-(acylamino)acrylates, poorer results were obtained with the corresponding (*Z*) stereoisomers (92-93% ee, see entries 2-5 and ref. [16]). It must be underlined that a decrease of the catalyst loading from 1% to 0.1% led to a drop in the enantioselectivity (entry 7).

Zheng and Kostas investigated the Rh-catalyzed hydrogenation of α-dehydroaminoacids derivatives **S3a**, **S3h-i** and

Table 4. Rh/ferrocene-based ligands L4a-L4l catalyzed hydrogenation of enamides S4a-e

Entry	Ligand	Substrate	Rh (mol %) [a]	Solvent	Time (h)[b]	e.e. (%)
1	**L4a**	**S4a**	1	THF [c]	-	87.5
2	**L4b**	**S4a**	1	CH_2Cl_2	1	10.6 (*R*)
3	**L4c**	**S4a**	1[d]	CH_2Cl_2	1	99.6 (*R*)
4	**L4d**	**S4a**	1	CH_2Cl_2	1	81.5 (*S*)
5	**L4e**	**S4a**	1	CH_2Cl_2	1	78.1 (*R*)
6	**L4f**	**S4a**	1	CH_2Cl_2	24	96.7 (*R*)
7	**L4g**	**S4a**	1	CH_2Cl_2	24	90.5 (*R*)
8	**L4h**	**S4a**	1	CH_2Cl_2	24	96.9 (*R*)
9	**L4j**	**S4a**	1	CH_2Cl_2	1	99.6 (*S*)
10	**L4k**	**S4a**	1	CH_2Cl_2	1	82.6 (*R*)
11	**L4l**	**S4a**	1	CH_2Cl_2	24	59.1 (*R*)
12	**L4c**	**S4b**	0.1	CH_2Cl_2	1	98.7 (*R*)
13	**L4c**	**S4c**	0.1	CH_2Cl_2	1	98.8 (*R*)
14	**L4c**	**S4d**	0.1	CH_2Cl_2	1	99.0 (*R*)
15	**L4c**	**S4e**	0.1	CH_2Cl_2	1	99.2 (*R*)

[a] Reactions were performed with a ligand/Rh ratio of 1.1. [b] In all cases, 100% conversion was achieved. [c] Reaction was conducted at 0°C, under 20 bars of H_2. [d] Similar result was obtained using 0.1 mol % of metal.

Table 5. Hydrogenation of itaconate S1a catalyzed by Rh/ferrocene-based ligands L4c, L4f-h and L4l complexes[a]

Entry	Ligand	Rh (mol %)	Time[b] (h)	e.e. (%)
1	**L4c**	0.1	0.5	99.9 (*S*)[c]
2	**L4f**	1	24	99.9 (*S*)
3	**L4h**	1	24	99.9 (*S*)
4	**L4g**	1	24	94.0 (*S*)
5	**L4l**	1	24	19.0 (*S*)

[a] The reactions were conducted at room temperature under an H_2 pressure of 10 bars. The catalyst was made in situ from $[Rh(cod)_2]BF_4$ and 1.1 equiv. of the ligand.
[b] In all cases, 100% conversion was achieved.
[c] A 99.1% ee value was obtained when 0.01 mol % catalyst was used.

S3k-l, respectively with diphenylphosphinoaryl-based ligands **L5a-d** and **L5f** (Scheme **11**, Table **7**) [18, 20]. The five ligands were tested in the hydrogenation of **S3a**. [(**L5f**)Rh(cod)]BF_4 complex proved to be very active since the reaction was completed in 10 minutes at room temperature under 1 bar of H_2 at 1.0 mol % catalyst loading (entry 5). The presence of the second stereogenic element in the matched ligand **L5d** slightly increased the enantioselectivity to 99.1% ee (entry 4). It is noteworthy that the configuration of the hydrogenated product was always (*R*), independently of the ligand **L5a-d** used (entries 1-4). This unexpected result points out that the absolute configuration of the product is not controlled by the chirality of the BINOL moiety but by the phenylethylamine moiety. Moreover, significantly decreasing the Rh-**L5d** catalyst loading to 0.01 mol % led to a non significant drop of the enantioselectivity (entry 6). It should also be noticed that the efficiency of the reaction depends on the nature of the solvent used [18, 20]. Finally, ligand **L5d** showed also excellent enantioselectivities in the Rh-catalyzed hydrogenation of compounds **S3h-i** and **S3k-l** (99.0 % ee to over 99.9% ee) [18].

Diphenylphosphinoaryl-based ligands **L5a-d** were also evaluated in the rhodium-catalyzed hydrogenation of enamides **S4a, S4c-h** (Scheme **12**, Table **8**) [18]. Reactions were conducted in the presence of 1.0 mol % of catalyst under 10 bars of H_2. Good to excellent enantioselectivities were obtained for the hydrogenation of **S4a**, **L5d** exhibiting the best selectivity (99.5% ee) (entry 4). Very high enantioselectivities (98.5-99.9% ee) were also observed in the Rh-**L5d** catalyzed hydrogenation of enamides **S4c-h** [18].

The catalytic performance of **L5a-d** and **L5f** was also investigated in the rhodium-catalyzed hydrogenation of dimethyl itaconate **S1a** (Scheme **14**, Table **9**) [18, 20]. In the presence of 1.0 mol % of complex [(**L5f**)Rh(cod)]BF_4, the dimethyl itaconate was reduced very rapidly to afford the

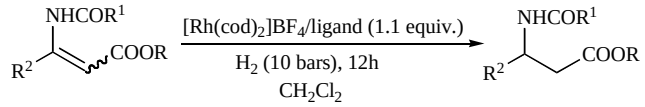

(*Z*)-**S5a** : R = Et, R^1 = Me, R^2 = Ph	**P5a**
(*Z*)-**S5b** : R = Et, R^1 = Me, R^2 = *p*-Me-Ph	**P5b**
(*Z*)-**S5c** : R = Me, R^1 = Me, R^2 = *p*-Me-Ph	**P5c**
(*Z*)-**S5d** : R = Et, R^1 = Me, R^2 = *p*-OMe-Ph	**P5d**
(*Z*)-**S5e** : R = Me, R^1 = Me, R^2 = *p*-OMe-Ph	**P5e**
(*Z*)-**S5f** : R = Et, R^1 = Me, R^2 = *p*-Cl-Ph	**P5f**
(*Z*)-**S5g** : R = Me, R^1 = Me, R^2 = *p*-Cl-Ph	**P5g**
(*Z*)-**S5h** : R = Me, R^1 = Me, R^2 = *p*-F-Ph	**P5h**
(*Z*)-**S5i** : R = Me, R^1 = Me, R^2 = m-OMe-Ph	**P5i**
(*Z*)-**S5j** : R = Me, R^1 = Me, R^2 = Me	**P5j**
(*E*)-**S5j** : R = Me, R^1 = Me, R^2 = Me	
(*Z*)-**S5k**: R = Et, R^1 = Me, R^2 = Me	**P5k**
(*E*)-**S5k** : R = Et, R^1 = Me, R^2 = Me	
(*Z*)-**S5l** : R = Me, R^1 = Ph, R^2 = Me	**P5l**
(*Z*)-**S5m** : R = Me, R^1 = Me, R^2 = Et	**P5m**
(*E*)-**S5m** : R = Me, R^1 = Me, R^2 = Et	
(*Z*)-**S5n** : R = Me, R^1 = Me, R^2 = *i*Pr	**P5n**
(*E*)-**S5n** : R = Me, R^1 = Me, R^2 = *i*Pr	

Scheme 13.

product in high ee (96.2%, entry 2). Using ligand **L5d** allowed for increasing the enantioselectivity to 99.9% ee (entry 1).

Zhang applied ligands **L7a-b** in the Rh-catalyzed hydrogenation of enamides **S4a, S4n-t** (Scheme **15**, Table **10**) [24b]. Rh/**7a**-catalyzed hydrogenation of **S4a** yielded the product with a high ee (99%, entry 1). When the catalyst loading was decreased to 0.1 mol %, only a minor deterioration in the ee was observed (98%, entry 1). The authors also noticed that the use of a more polar or protic solvent led to a drop in the enantioselectivity [24b]. The reduction of enamides **S4e** and **S4i-m** also afforded products with high ee values (96-99%) [24b]. The efficiency of ligands **L7a-b** was also tested in the reduction of hindered *ortho*-substituted arylenamides **S4n-S4t** (entries 2-10). Very interesting results were obtained for these difficult substrates as, for each enamide, the ee value was higher than the best ee value reported in the literature [24b].

The performance of ligands **L7a-d** was also investigated in the rhodium-catalyzed hydrogenation of α-dehydroamino acid esters **S2**, **S3a**, **S3h-i and S3l-r** (Scheme **11**, Table **11**) [24a]. Solvent optimization in the Rh/**L7a** catalyzed hydrogenation of **S3a** revealed acetone and MEK to be superior to many other solvents [24a]. Several compounds were then tested in the reaction with each of the four ligands and the best of the four results is given in Table **11**. Both aromatic and aliphatic substrates were hydrogenated with high to very high enantioselectivities (96.8-99.4% ee), the nature of the best ligand being dependant on the substrate.

The catalytic performance of ligands **L7a-d** was also tested in the Rh-catalyzed hydrogenation of itaconates **S1a-d** (Scheme **16**, Table **12**) [24a]. Various solvents were

Table 6. Hydrogenation of β-(acylamino)acrylates S5a-S5n catalyzed by Rh/ferrocene-based ligands L4c and L4i complexes[a]

Entry	Ligand	Substrate	Rh (mol %)	Temperature (°C)	e.e. (%)
1	**L4c**	**(*Z*)-S5a**	1.0	RT	65
2	**L4i**	**(*Z*)-S5a**	1.0	5	>99 (*R*)
3	**L4i**	**(*Z*)-S5a**	0.1	5	98 (*R*)
4	**L4i**	**(*Z*)-S5j**	1.0	5	92 (*S*)
5	**L4i**	**(*E*)-S5j**	1.0	5	98 (*R*)
6	**L4i**	**(*E*)-S5m**	1.0	5	99 (*R*)
7	**L4i**	**(*E*)-S5m**	0.1	5	95 (*R*)

[a] In all cases, 100% conversion was achieved.

Table 7. Rh/L5a-d and Rh/L5f-catalyzed hydrogenation of α-dehydroamino acid derivative S3a[a]

Entry	Ligand	Substrate	Ligand/Rh (mol %)	Pressure (bar)	Time (h)[b]	e.e. (%)
1	**L5a**	**S3a**	1.1/1.0	10	12	17.3 (*R*)
2	**L5b**	**S3a**	1.1/1.0	10	12	98.1 (*R*)
3	**L5c**	**S3a**	1.1/1.0	10	12	48.5 (*R*)
4	**L5d**	**S3a**	1.1/1.0	10	12	99.1 (*R*)
5	**L5f**	**S3a**	1.0[c]	1	0.167	97.9 (*S*)
6	**L5d**	**S3a**	0.011/0.01	10	12	98.8 (*R*)

[a] Reactions were carried out in CH_2Cl_2. [b] Complete conversion was obtained in all reactions. [c] Isolated [(**L5f**) Rh(cod)]BF_4 complex was used.

Table 8. Rh/L5a-d catalyzed hydrogenation of enamide S4a[a, b,c]

Entry	Ligand	e.e. (%)
1	**L5a**	95.9 (*R*)
2	**L5b**	98.6 (*R*)
3	**L5c**	73.9 (*R*)
4	**L5d**	99.5 (*R*)

[a] All reactions were carried out with 1 mol % of [Rh(cod)]BF_4 and 1.1 mol % of ligand.
[b] In all cases, reactions were conducted for 12h and 100% conversion was achieved.
[c] CH_2Cl_2 was used as the solvent.

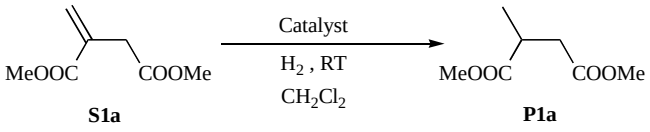

S1a **P1a**

Scheme 14.

Table 9. Rh/L5d and Rh/L5f catalyzed hydrogenation of itaconate S1a[a]

Entry	Catalyst (mol %)	H_2 Pressure (bar)	Time (h)	e.e. (%)
1	$Rh(cod)_2BF_4$/**L5d** (1)[b]	10	12	99.9
2	[(**L5f**)Rh(cod)]BF_4 (1)[c]	1	0.43	96.2 (*R*)

[a] Complete conversion was obtained in all reaction.
[b] Catalyst was prepared in situ with 1.1 equiv. of ligand **L5d**.
[c] Isolated [(**L5f**) Rh(cod)]BF_4 complex was used.

screened in the Rh/**L7a**-catalyzed hydrogenation of compounds **S1a-d**. Emphasizing the key role of the solvent in this reaction, it was observed that both the enantioselectivity

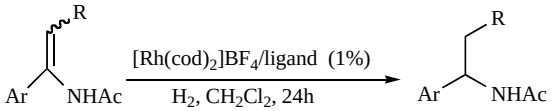

S4a : Ar = Ph, R = H	**P4a**
S4e : Ar = *p*-CF_3-Ph, R = H	**P4e**
S4i : Ar = *p*-CF_3-Ph, R = Me	**P4i**
S4j : Ar = *m*-Me-Ph, R = H	**P4j**
S4k : Ar = *p*-MeO-Ph, R = Me	**P4k**
S4l : Ar = 2-naphtyl, R = H	**P4l**
S4m : Ar = 2-naphtyl, R = Me	**P4m**
S4n : Ar = *o*-Me-Ph, R = H	**P4n**
S4o : Ar = *o*-MeO-Ph, R = H	**P4o**
S4p : Ar = *o*-F-Ph, R = H	**P4p**
S4q : Ar = *o*-Cl-Ph, R = H	**P4q**
S4r : Ar = *o*-NO_2-Ph, R = H	**P4r**
S4s : Ar = *o*-CF_3-Ph, R = H	**P4s**
S4t : Ar = 1-naphthyl, R = H	**P4t**

Scheme 15.

and the absolute configuration were solvent dependant. The results obtained with dimethyl itaconate **S1a** are given in entries 1-8. This unusual result may be explained by the involvement of the solvent in key enantiodifferentiating steps. Reactions were also carried out with each of the four ligands under the best conditions. The best of the four results is given for each substrate in entries 8-11. Very high enantioselectivities (98.8-99.6% ee) were obtained with each itaconate, the best ligand being either **L7a** or **L7d**.

The Rh-catalyzed hydrogenation of β-aryl enol ester phosphonates **S6a-k** was recently examined by Zheng, using ligands **L5h-i** (Scheme **17**, Table **13**) [22]. Excellent enantioselectivities (99.2-99.9% ee) were obtained regardless of

Table 10. Hydrogenation of enamides S4a, S4n-t catalyzed by Rh/L7a-b[a]

Entry	Ligand	Substrate	Temperature (°C)/ H_2 Pressure (bar)	e.e. (%)
1	**L7a**	**S4a**	RT/ 1	99 (*R*)[b]
2	**L7a**	**S4n**	RT/ 5	84.0 (*R*)
3	**L7a**	**S4n**	0/ 25	91.0 (*R*)
4	**L7a**	**S4o**	RT/ 5	99.4 (*R*)
5	**L7a**	**S4p**	RT/ 5	99.0 (*R*)
6	**L7a**	**S4q**	RT/ 5	99.6 (*R*)
7	**L7a**	**S4r**	RT/ 5	98.2 (n.c.)
8	**L7b**	**S4s**	RT/ 5	94.2 (n.c.)
9	**L7b**	**S4t**	RT/ 5	92.8 (*R*)
10	**L7b**	**S4t**	RT/ 5	93.8 (*R*)[c]

[a] In all reactions, full conversion was obtained. [b] A 98% ee value was obtained at a 0.1 mol % catalyst loading. [c] 2,2,2-trifluoroethanol was used as solvent.

the substrate (entries 1-3 and [22]) when the matched ligand (*Rc*, *Ra*)-**L5h** was used in CH_2Cl_2 or in *i*PrOH. It has to be noticed that the ee value was not affected when **S6a** was hydrogenated under a lower catalyst loading (0.1 mol %, entry 1). Interestingly, the authors observed that the formation of the chiral carbon in the product was mainly controlled by the chiral carbon of the tetrahydronaphtylamine moiety (compare results of entries 1 and 2). The study was extended to β-alkoxy enol ester phosphonates **S6l-n**, β-alkyl-substituted and β-unsubstituted enol ester phosphonates **S6o-q**. Again, excellent ee values were obtained for all substrates (98.9-99.9% ee, entries 4-6 and [22]). It is worth noting that the enantioselectivity and the conversion were not altered when **S6o** was hydrogenated in the presence of a lower catalyst loading (0.1 mol %, entry 5). It must be underlined that the enantioselectivities obtained with ligand **L5h** are the best reported to date in the hydrogenation of this familly of challenging substrates.

2.1.3.2. Ru-catalyzed Asymmetric Hydrogenation of Aromatic Ketones [12b]

When ligands **L1a** or **L1b** were used in the presence of diamine **26** as the co-catalyst, acetophenone **S7a** was converted, after 16h, respectively to (*S*) and (*R*) isomers of alcohol **P7a** with good conversions and moderate to good enantioselectivities (Scheme **18**, Table **14**, entries 1 and 2). An increase in the conversion was obtained when the reaction was carried out in the presence of chiral diamine **27** instead of diamine **26** (entries 3, 4). However, the use of the **L1a**/**27** combination led to a significant drop in the ee value (6% ee, entry 3) while the use of the **L1b**/**27** system resulted in a high ee value (94% ee, entry 4). It clearly appears that the former combination matched worse while the latter matched best among all four possibilities (entries 3-6). It is interesting to underline that the formation of the chiral carbon in the product is mainly controlled by the chiral carbon of the dihydroquinoline moiety (compare product configurations in entries 1-2 and entries 3-6). Finally, similar results were obtained with substrates **S7b** and **S7c** [12b].

Table 11. Rh/L7a-d catalyzed hydrogenation of α-dehydroamino esters S2, S3a, S3h-i and S3l-r[a]

Entry	Ligand	Substrate	e.e. (%)
1	**L7c**	**S3a**	98.8 (*R*)
2	**L7b**	**S3h**	97.0 (*R*)
3	**L7d**	**S3i**	98.2 (*R*)
4	**L7c**	**S3l**	99.4 (*R*)
5	**L7c**	**S3m**	98.4 (*R*)
6	**L7c**	**S3n**	98.4 (*R*)
7	**L7a**	**S3o**	97.4 (*R*)
8	**L7d**	**S3p**	96.8 (*R*)
9	**L7d**	**S3q**	99.2 (*R*)
10	**L7d**	**S3r**	96.8 (*R*)
11	**L7d**	**S2**	99.2 (*R*)

[a] Reactions were performed with 1.0 mol % of the catalyst, under 1 bar of H_2 pressure at room temperature for 18h in acetone. A full conversion was obtained in all reactions.

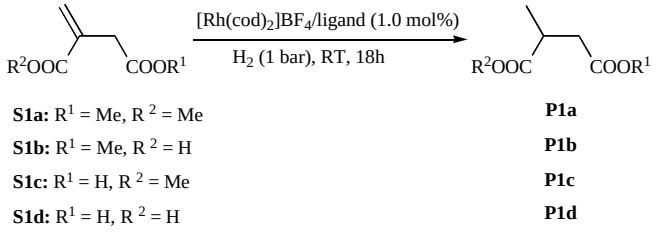

Scheme 16.

Table 12. Hydrogenation of itaconates S1a-d catalyzed by Rh/L7a-d[a]

Entry	Ligand	Substrate	Solvent	e.e. (%)
1	**L7a**	**S1a**	CH_2Cl_2	96.6 (*R*)
2	**L7a**	**S1a**	toluene	3.0 (*R*)
3	**L7a**	**S1a**	THF	10.4 (*R*)
4	**L7a**	**S1a**	AcOEt	11.6 (*S*)
5	**L7a**	**S1a**	acetone	39.6 (*S*)
6	**L7a**	**S1a**	MEK	30.4 (*S*)
7	**L7a**	**S1a**	MeOH	32.0 (*R*)
8	**L7a or L7d**	**S1a**	TFE	99.2 (*R*)
9	**L7d**	**S1b**	TFE	99.6 (*R*)
10	**L7a**	**S1c**	TFE	98.8 (*R*)
11	**L7d**	**S1d**	TFE	99.6 (*R*)

[a] Complete conversion was obtained in all reactions except for reactions of entries 2, 4 and 7.

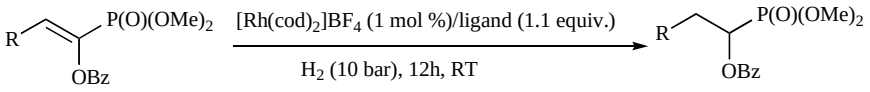

S6a : R = Ph	**P6a**
S6b : R = *p*-F-Ph	**P6b**
S6c : R = *p*-Cl-Ph	**P6c**
S6d : R = *p*-Br-Ph	**P6d**
S6e : R = *p*-NO_2-Ph	**P6e**
S6f : R = *p*-MeO-Ph	**P6f**
S6g : R = *m*-MeO-Ph	**P6g**
S6h : R = *m*-Cl-Ph	**P6h**
S6i : R = *o*-Cl-Ph	**P6i**
S6j : R = 1-naphtyl	**P6j**
S6k : R = 2-thienyl	**P6k**
S6l : R = OMe	**P6l**
S6m : R = OEt	**P6m**
S6n : R = O*i*Pr	**P6n**
S6o : R = H	**P6o**
S6p : R = Me	**P6p**
S6q : R = Et	**P6q**

Scheme 17.

Table 13. Rh/L5h-i catalyzed hydrogenation of β-alkyl- and β-aryl enol ester phosphonates S6a-q[a]

Entry	Ligand	Substrate	Solvent	e.e. (%)
1	**L5h**	**S6a**	CH_2Cl_2	99.4[b]
2	**L5i**	**S6a**	CH_2Cl_2	60.3[c]
3	**L5h**	**S6a**	*i*PrOH	99.5
4	**L5h**	**S6l**	CH_2Cl_2	99.7
5	**L5h**	**S6o**	*i*PrOH	99.5[b]
6	**L5h**	**S6q**	*i*PrOH	99.9

[a] Complete conversion was observed for all reactions.
[b] A similar result was obtained when the catalyst loading was decreased to 0.1 mol %.
[c] The major enantiomer was the same in the reactions of entries 1 and 2.

2.1.3.3. Hydroformylation

The organotransition metal-catalyzed enantioselective hydroformylation of alkenes is a very challenging reaction and only few efficient catalysts have been reported for this reaction [19]. Diastereoisomeric ligands **L1a** and **L1b** were evaluated towards Rh-catalyzed hydroformylation of styrene **S8a** (Scheme **19**) [12a]. The reaction gave, with both ligand, a mixture of the linear and the branched aldehyde in favour of the latter in high regioselectivity. However, the (*Rc*,*Ra*)-**L1a** and (*Sc*,*Ra*)-**L1b** ligands gave aldehyde **P8a** respectively with a poor (4.8%) and a somewhat high (74.0%) ee.

Reek considered the synthesis of **P8a** by Rh/**L3a-d** catalyzed hydroformylation of styrene (Scheme **20**, Table **15**) [13]. A high regioselectivity (17/1) in favour of the branched isomer **P8a** was obtained with **L3b** but the ee was moderate (50%) and the conversion was not complete after 65h (entry 2). On the other hand, a nearly full conversion was observed with ligand **L3d** and the isomer **P8a** was isolated with a rather good ee value (72%, entry 4). Very poor results were obtained with ligands **L3a** and **L3c** (entries 1 and 3).

Ligand **L5e** was tested in the Rh-catalyzed hydroformylation of styrenes **S8a-g** and vinyl acetate **S8h** (Scheme **20**, Table **16**) [19]. The reaction was first studied on styrene **S8a**. Search for optimal conditions showed that the enantioselectivity was affected by the nature of the solvent and the temperature but not by the total pressure. Nevertheless, a drop in the reaction rate was observed at higher pressure (entry 2). Under the optimized reaction conditions (entry 1), a complete conversion was observed, the mixture of aldehydes was obtained with moderate regioselectivity and an unprece-

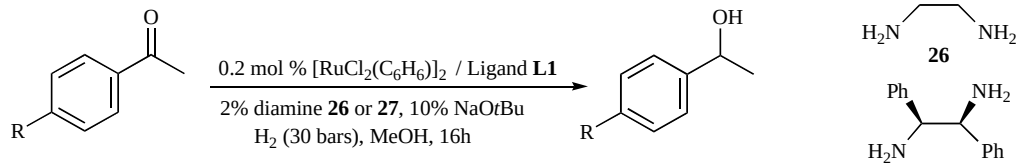

S7a : R = H **P7a**
S7b : R = F **P7b**
S7c : R = OMe **P7c**

Scheme 18.

Table 14. Ru/QUINAPHOS-catalyzed asymmetric hydrogenation of acetophenone S7a

Entry	Ligand	Diamine	Conv. (%)	e.e. (%)
1	**L1a**	**26**	91	65 (*S*)
2	**L1b**	**26**	90	80 (*R*)
3	**L1a**	**27**	>99	6 (*R*)
4	**L1b**	**27**	>99	94 (*R*)
5	**L1c**	**27**	>99	36 (*S*)
6	**L1d**	**27**	>99	75 (*R*)

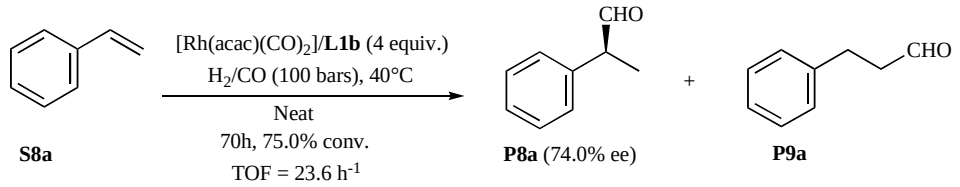

S8a **P8a** (74.0% ee) **P9a**

P8a/**P9a** : 96.7/3.3

Scheme 19.

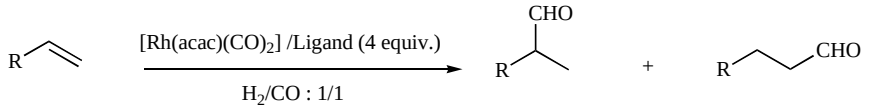

S8a : R = Ph	**P8a**	**P9a**
S8b : R = *p*-Me-Ph	**P8b**	**P9b**
S8c : R = *p*-F-Ph	**P8c**	**P9c**
S8d : R = *o*-F-Ph	**P8d**	**P9d**
S8e : R = *p*-Cl-Ph	**P8e**	**P9e**
S8f : R = *p*-MeO-Ph	**P8f**	**P9f**
S8g : R = *p*-*i*Bu-Ph	**P8g**	**P9g**
S8h : R = OAc	**P8h**	**P9h**

Scheme 20.

Table 15. Rh/L3a-d catalyzed hydroformylation of styrene S8a[a]

Entry	Ligand	Time (h)	Temp. (°C)	Conv. (%)	P8a/P9a	e.e. (%)
1	**L3a**	48	60	3	2	0
2	**L3b**	65	40	84	17	50 (*R*)
3	**L3c**	19	60	99	12	9 (*R*)
4	**L3d**	19	40	96	10	72 (*R*)

[a] Reactions were conducted in toluene with 0.1 mol % of catalyst under 10 bars of pressure.

dented very high enantioselectivity was reached for the branched isomer **P8a** (98% ee). It must be noted that racemization of the product was very low under the reaction conditions as the ee was only lowered from 98% to 97% when the reaction time was increased from 24h to 36h (entry 3). It is also worth noting that the catalytic system remained very efficient when the catalyst loading was decreased to 0.01 mol % (entry 4). Under these conditions, the enantioselectivity was not altered and the conversion was only slightly diminished to 89%. The reaction was also performed under optimized conditions with various substituted styrenes **S8b-g**. No influence of the substituant on the aromatic ring was noticed since regioselectivities were in the range of 86/14-91/9 and enantioselectivities were high for all substrates tested (98-99% ee). When vinyl acetate **S8h** was engaged in the reaction, a drop in the conversion and a slight decrease in the enantioselectvity were observed (entry 5).

Table 16. Rh/L5e-catalyzed hydroformylation of styrene S8a and vinyl acetate S8h[a]

Entry	Substrate	H_2/CO Pressure (atm)	Time (h)	Conv. (%)	P8/P9	e.e. (%)
1	**S8a**	10/10	24	>99	88/12	98 (*R*)
2	**S8a**	30/30	24	83	88/12	98 (*R*)
3	**S8a**	10/10	36	>99	88/12	97 (*R*)
4[b]	**S8a**	10/10	24	89	88/12	98 (*R*)
5	**S8h**	10/10	24	75	93/7	96 (*S*)

[a] Reactions were performed in benzene with a catalyst loading of 0.1 mol % at 60°C.
[b] Catalyst loading of 0.01 mol %.

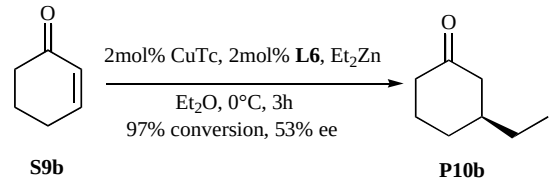

S9b **P10b**

Scheme 21.

2.1.3.4. Cu-Catalyzed Conjugate Addition on Enones

Ligand **L6** was evaluated in the Cu-catalyzed conjugate addition of diethylzinc to cyclohexenone **S9b** (Scheme **21**) [23]. A nearly complete conversion was obtained after 3h at 0°C, but the enantioselectivity was moderate with a ee value of 53%.

2.2. Phosphoramidite-Phosphite Ligands

2.2.1. Overview

Monodentate phosphoramidites and monodentate phosphites constitute two efficient classes of chiral ligands which induce good enantioselectivities in a wide range of transformations. Indeed, efforts focused on the combination of those two chelating groups have allowed for the synthesis of various hybrid bidentate phosphoramidite-phosphite ligands. The synthesis of such compounds requires the use of amino alcohols to provide, in one hand the phosphoramidite moiety and on the other hand the phosphite moiety, by reaction with various chlorophosphites. Thus, different structures have been designed from sugars, α-amino acids, ephedrine and tropanes skeletons.

2.2.2. Synthesis of Phosphoramidite-Phosphite Ligands

The first synthesis of a phosphoramidite-phosphite ligand was reported by Agbossou and co-workers in 2000 [29]. Compounds **L8a-L8d** were straightforwardly prepared by treatment of ephedrine with an excess of various chlorophosphites in presence of triethylamine. After filtration through a basic alumina plug, this straightforward synthesis afforded compounds **L8a-L8d** with moderate to good yields (Scheme **22**).

Subsequently to this first report, the same group published the synthesis of prolinol-based phosphoramidite-phosphites [30]. Following a similar procedure than the one used before, new unsymmetrical ligands were isolated in high yields (Scheme **23**). However, it was found that ligand **L9** was less stable than **L10** because of the fragility of its P—N bond.

This strategy was later used by the group of Cesarotti to synthesize BINOL-containing analogues **L11** and **L12** (Scheme **24**) [31].

Moreover, Diéguez and co-workers designed a series of phosphoramidite-phosphite ligands based on a furanoside

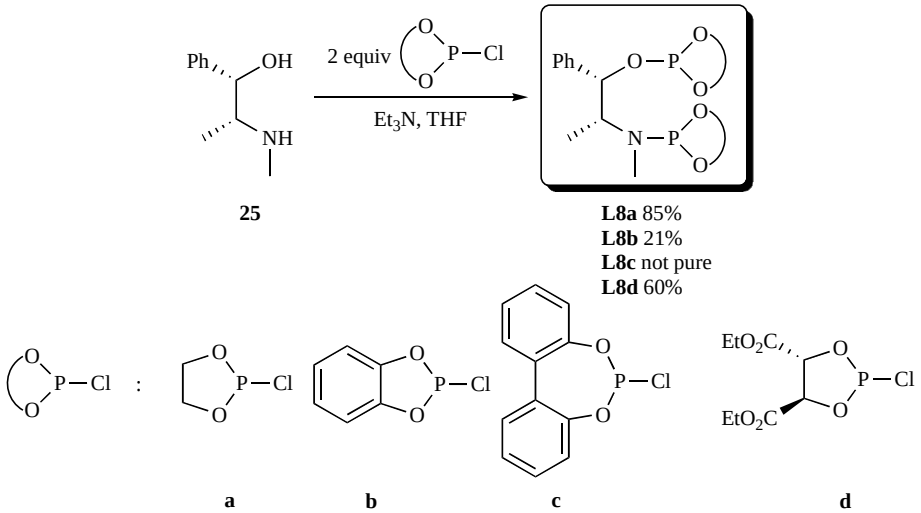

Scheme 22.

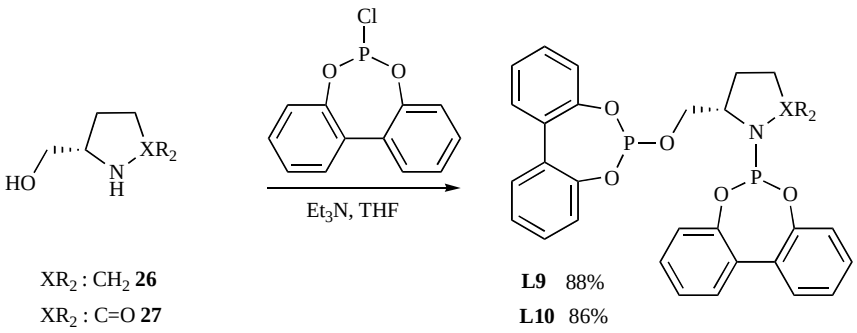

Scheme 23.

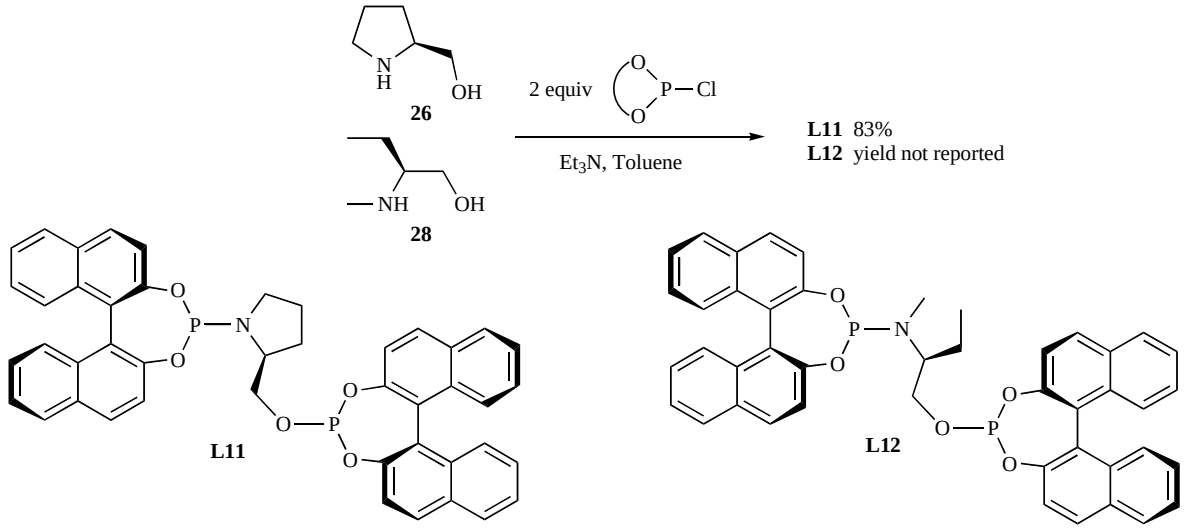

Scheme 24.

backbone [32, 33, 34a]. Ligands **L13-L16** were efficiently synthesized from the corresponding amino alcohols **29** and **30**, which could be easily obtained from inexpensive D-(+)-xylose [34b-c]. The reaction of these compounds in the presence of pyridine with two equivalents of the desired in situ formed chlorophosphite produced ligands **L13-L16** in good overall yields (Scheme **25**).

The BINOL-containing counterparts **L17-L18** have been synthesized using the same strategy with lower yields (Scheme **26**) [35].

Few years later, the synthesis of pyranoside analogues was also reported. Starting from D-Glucosamine and using the strategy previously described, ligands **L19a-L19c**, which exhibit different steric and electronic properties, were prepared (Scheme **27**) [36b, 37].

Hybrid phosphoramidite-phosphite based on a tropane skeleton have been reported by the group of Laschat (Scheme **28**) [38]. The key amino alcohol **35** was obtained in a five-step procedure. Tropinone **34** was prepared via [4+3] cycloaddition of N-protected pyrrol **32** with tetrabromoacetone **33**. Then, acetalization of ketone **34** was followed by an enantioselective hydroboration which afforded a N-protected amino alcohol. Finally, a catalytic hydrogenation gave the free amino alcohol **35**, precursor for the ligand synthesis. Treatment of compound **35**, in presence of triethylamine and catalytic amounts of DMAP at room temperature, with BINOL-derived chlorophosphites provided the desired ligands **L20a-b** in good yields. It is noteworthy that the preparation of H8-BINOL derived counterparts **L20c** and **L20d** was more difficult to carry out. Indeed, an alternative method using *n*-BuLi had to be used for the deprotonation of **35** before the addition of H8-BINOL-derived chlorophosphites and even under these conditions, only low yields were obtained.

2.2.3. Evaluation of Phosphoramidite-Phosphite Ligands in Asymmetric Catalysis

The ligands previously described have been involved in various asymmetric transformations catalyzed by transition metals. An overview of these reactions will be presented in the next sections.

2.2.3.1. Hydrogenation of Carbon-Carbon Double Bonds

Ligands **L11**, **L13-16** and **L20a-d** have been evaluated in the Rh-catalyzed hydrogenation of β-(acylamino)acrylates (Scheme **29**, Table **17**) [31, 34a, 38]. In a general manner, phosphoramidite-phosphite **L11** was not found very efficient for the reduction of **S3a** and **S11**. Only low enantioselectivities were observed ranging from 59 to 67% (entries 1-3). However, sugar based-ligands developed by Diéguez and coworkers showed good results in this transformation and also for the hydrogenation of itaconate derivatives (Scheme **30**, Table **18**). A thorough evaluation of the catalytic activity of

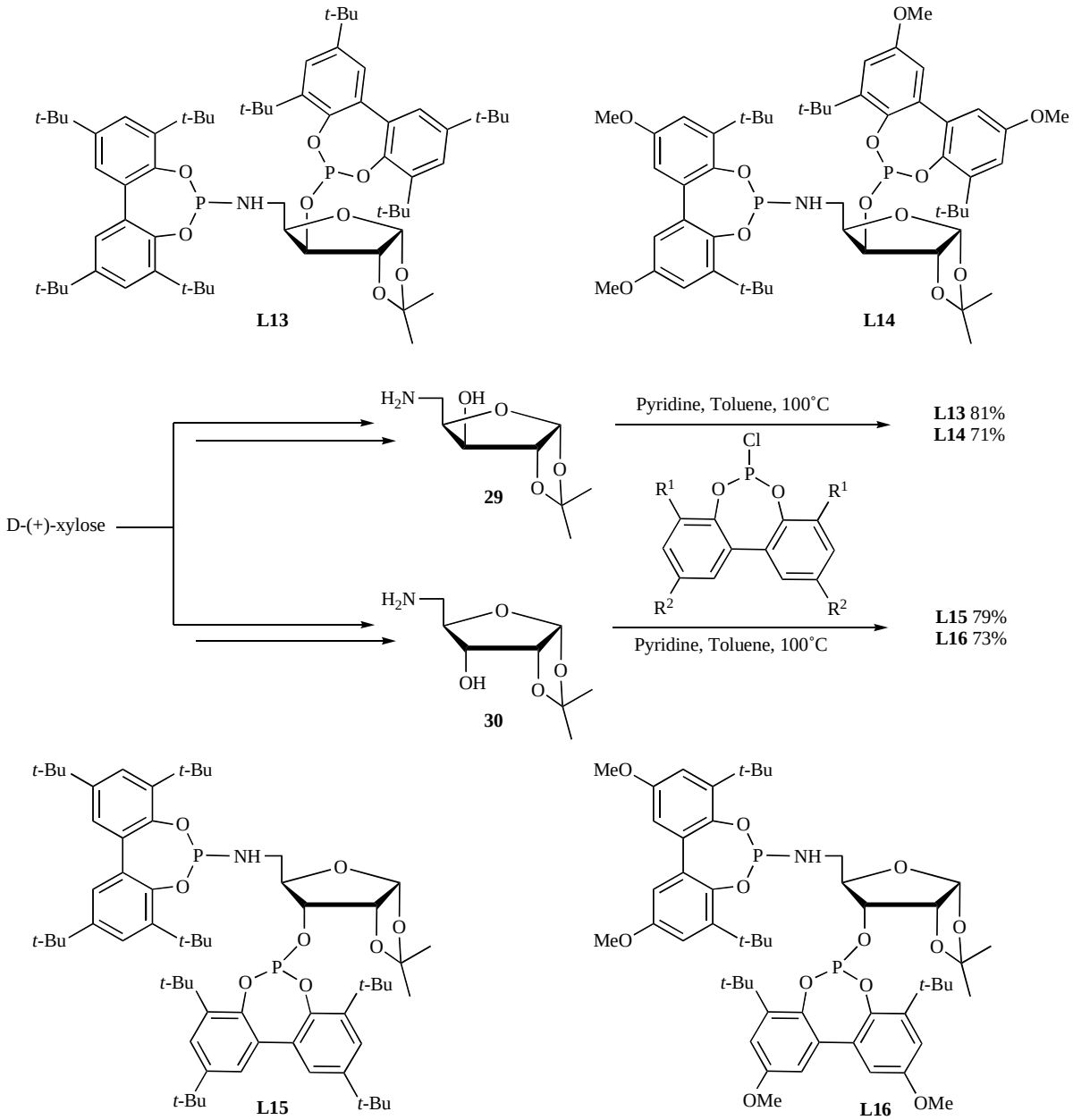

Scheme 25.

L13-16 highlighted that the chiral induction was strongly dependent of the carbohydrate backbone C3 stereocenter. A *S* configuration at C3 and *tert*-butyl groups in both *ortho* and *para* positions of the biphenyl moieties was the best combination to reach high enantioselectivities (Table **17**, entries 4-7 and Table **18**, entries 2-5). Interestingly, tropane-based ligands and especially **L20a** led to good results with regard to yield and selectivity even under only 1 bar of hydrogen pressure (Table **17**, entry 14 and Table **18**, entry 9). However, it is noteworthy that phosphoramidite-phosphite ligands seem to be slightly less efficient than their phosphine-containing counterparts for this transformation.

2.2.3.2. Hydroformylation

The rhodium-catalyzed hydroformylation of styrene represents the first application of phosphoramidite-phosphite ligands in asymmetric catalysis (Scheme **31**, Table **19**) [29]. Ligands **L8a,b,d** induced regioelectivities ranging from 60 to 90 % in favour of the branched product **P8a** but only displayed poor enantioselectivities (Table **19**, entries 1-3). Additionally, the evaluation of **L9** under similar reaction conditions afforded also modest results (Table **19**, entries 4 and 5) [30]. Ligands **L13-16** based on a furanoside backbone were successfully applied to this reaction improving significantly the regioselectivity and the chiral induction (Table **19**, entries 6-12) [32]. Indeed, 96 to 97% of branched product **P8a** was obtained with enantiomeric excesses up to 65%. The authors also highlighted that partial pressures of CO and H_2 influenced the catalytic activity in terms of TOF; higher partial pressures of H_2 leading to better conversion values (Table **19**, entries 6-8). Moreover, variations of the ligand / rhodium ratio showed that these catalytic systems are highly

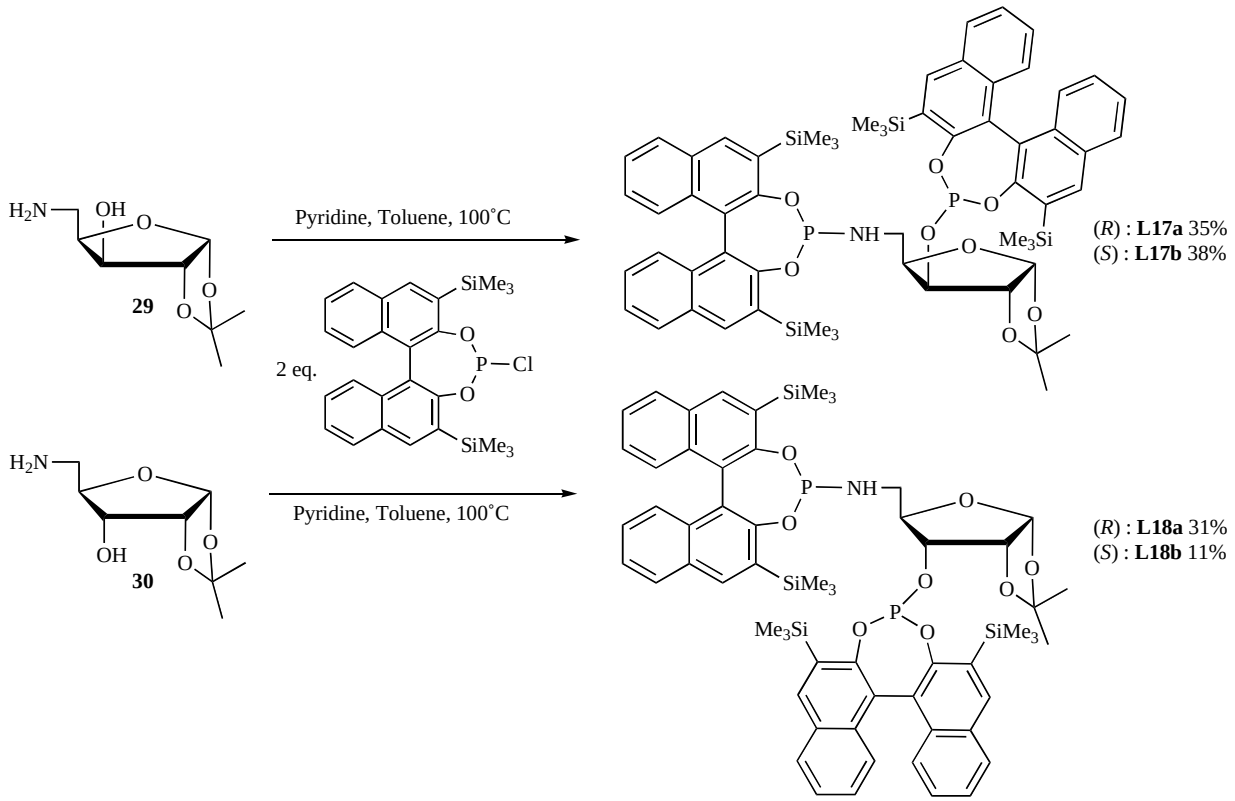

Scheme 26.

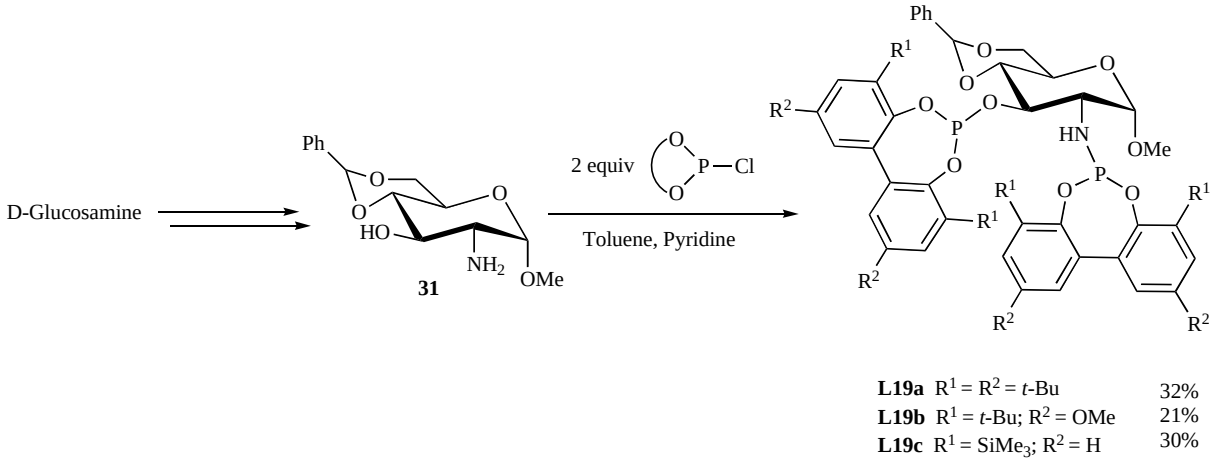

Scheme 27.

stable under hydroformylation conditions and that no excess of ligand is required (Table **19**, entry 9). Nevertheless, it should be noted that once again phosphoramidite-phosphine ligands seem to be better tools for this transformation.

Ligand **L11** was also applied to rhodium-catalyzed hydroformylation reaction of vinylacetate **S8h** (Scheme **32**) [31]. The branched product **P8h** was obtained with a good regio- albeit a poor enantioselectivity.

Stable platinum complexes bearing ligand **L9** were evaluated in the hydroformylation of styrene (Scheme **33**, Table **20**) [30]. Only modest enantioselectivities (30-44% e.e.) and regioselectivities were observed. Additionnally, undesired by-products of hydrogenation reaction were detected in quite large amounts (20-35%).

2.2.3.3. Cu-Catalyzed Conjugate Addition on Enones

Encouraged by the success of monodentate phosphoramidite and phosphite ligands in the copper-catalyzed conjugate addition reaction, several groups developed and tested hybrid ligands bearing these two functionalities for this process. Thus, the conjugate addition of diethylzinc to cyclohexenone **S9b** using furanoside-containing ligand **L13** was studied in 2001 by Diéguez and co-workers (Scheme **34**) [33]. Unfortunately, only 30% e.e. was reached under these conditions. More recently, the same group reported a

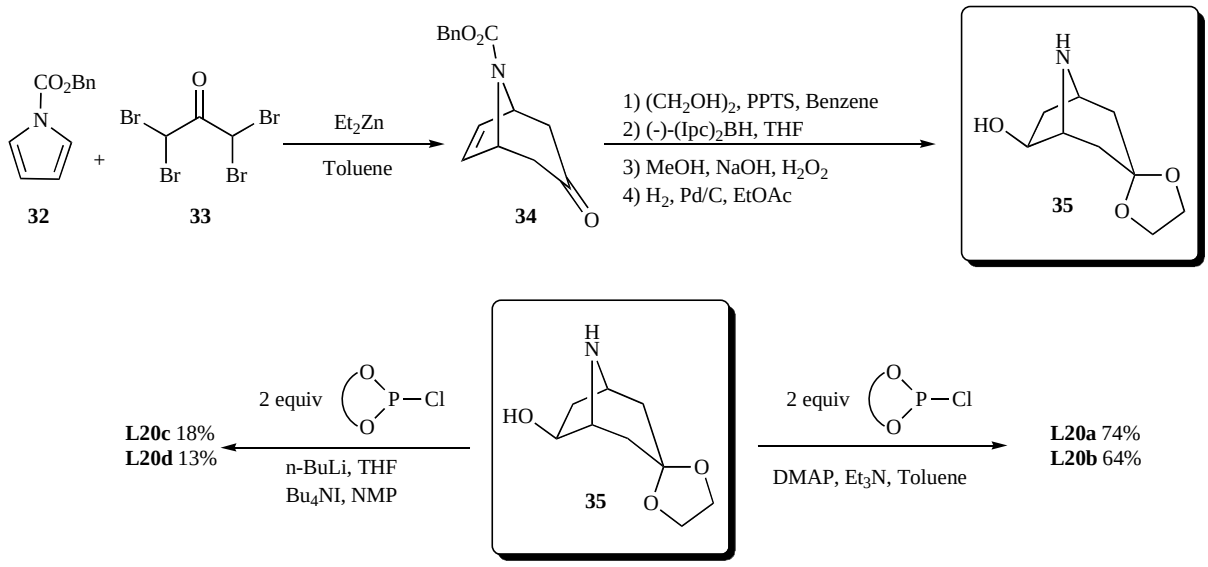

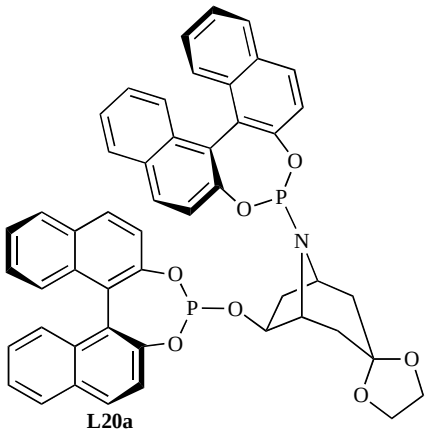

L20a

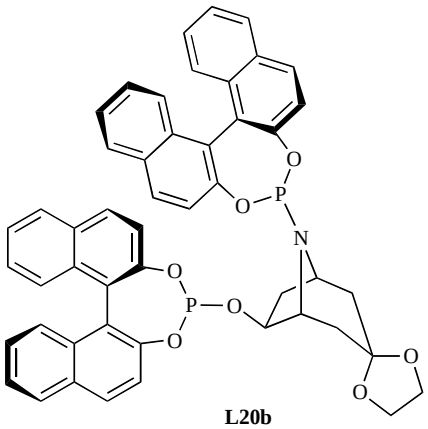

L20b

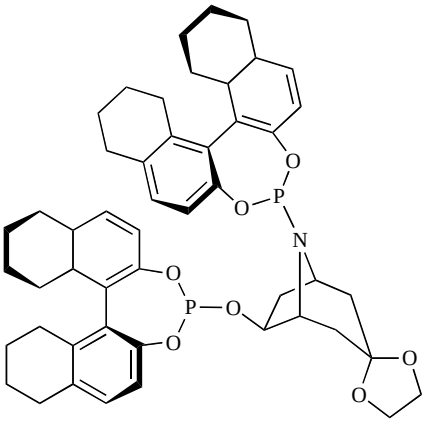

L20c

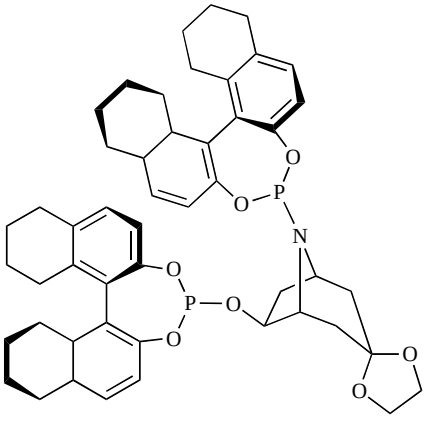

L20d

Scheme 28.

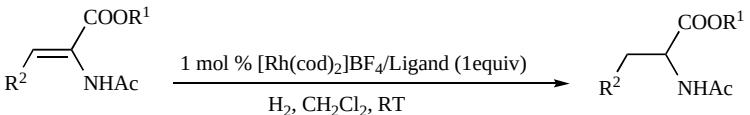

S3a : R^1 = CH_3, R^2 = Ph — **P3a**

S2 : R^1 = CH_3, R^2 = H — **P2**

S11 : R^1 = H, R^2 = Ph — **P12**

Scheme 29.

Table 17. Hydrogenation of β-(acylamino)acrylates catalyzed by rhodium/ phosphoramidite-phosphite complexes

Entry	Ligand	Substrate	Pressure (bar)	Time (h)	Conv. (%)	e.e. (%)
1[a]	**L11**	**S3a**	10	1.5	100	63 (*R*)
2[a,b]	**L11**	**S3a**	100	1	100	67 (*R*)
3[a]	**L11**	**S11**	1	6	100	59 (*R*)
4	**L13**	**S3a**	5	8	77	94 (*S*)
5[c]	**L13**	**S3a**	30	12	72	98 (*S*)
6	**L13**	**S2**	5	8	100	92 (*S*)
7[c]	**L13**	**S2**	30	12	100	98 (*S*)
8	**L14**	**S3a**	5	8	53	85 (*S*)
9	**L14**	**S2**	5	8	71	82 (*S*)
10	**L15**	**S3a**	5	8	29	18 (*S*)
11	**L15**	**S2**	5	8	46	15 (*S*)
12	**L16**	**S3a**	5	8	35	17 (*S*)
13	**L16**	**S2**	5	8	33	12 (*S*)
14	**L20a**	**S3a**	1	12	100	95 (*R*)
15	**L20b**	**S3a**	1	12	100	85 (*S*)
16	**L20c**	**S3a**	1	12	100	88 (*R*)
17	**L20d**	**S3a**	1	12	100	84 (*S*)

[a] Reaction performed in THF. [b] Reaction performed at 0ºC. [c] Reaction performed at 5ºC.

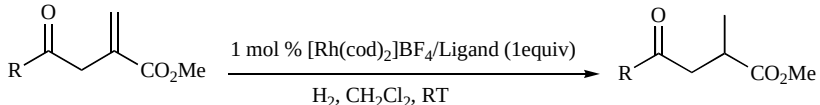

S1a : R = OCH_3
S10 : R = CH_3

P1a
P11

Scheme 30.

Table 18. Hydrogenation of itaconate derivatives catalyzed by Rhodium/ phosphoramidite-phosphite complexes

Entry	Ligand	Substrate	Pressure (bar)	Time (h)	Conv. (%)	e.e. (%)
1	**L13**	**S10**	1	20	100	65 (*R*)
2	**L13**	**S10**	5	8	100	96 (*R*)
3	**L13**	**S10**	30	1.5	100	97 (*R*)
4[a]	**L13**	**S10**	30	10	100	97 (*R*)
5[b]	**L13**	**S10**	30	12	100	>99 (*R*)
6	**L14**	**S10**	5	8	86	86 (*R*)
7	**L15**	**S10**	5	8	46	34 (*R*)
8	**L16**	**S10**	5	8	40	30 (*R*)
9	**L20a**	**S1a**	1	12	100	85 (*S*)
10	**L20b**	**S1a**	1	12	100	62 (*R*)
11	**L20c**	**S1a**	1	12	100	80 (*S*)
12	**L20d**	**S1a**	1	12	100	17 (*R*)

[a] Catalyst loading 0.1 mol %. [b] Reaction performed at 5ºC.

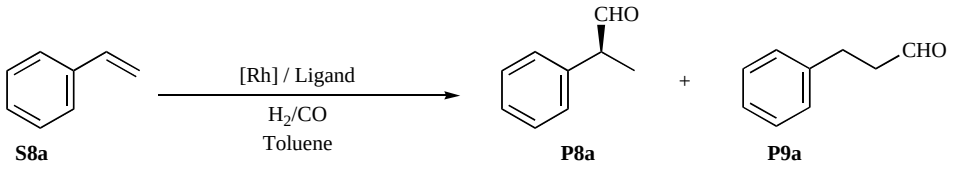

Scheme 31.

Table 19. Hydroformylation of styrene catalyzed by rhodium/ phosphoramidite-phosphite complexes

Entry	Ligand	Time (h)	Temp. (°C)	Conv. (%)	P8a/P9a	e.e. (%)
1[a]	**L8a**	48	80	100	9	8 (*R*)
2[a]	**L8b**	48	80	45	1.5	5 (*R*)
3[a]	**L8d**	48	80	94	4	8 (*R*)
4[a]	**L9**	48	80	100	1.7	5 (*S*)
5[a]	**L9**	48	40	15	7.3	19 (*S*)
6[b]	**L13**	24	40	68	32.3	35 (*S*)
7[b,c]	**L13**	24	40	46	32.3	36 (*S*)
8[b,d]	**L13**	24	40	35	32.3	35 (*S*)
9[b,e]	**L13**	24	40	69	32.3	36 (*S*)
10[b]	**L14**	24	40	83	24	55 (*S*)
11[b]	**L15**	24	40	100	24	15 (*S*)
12[b]	**L16**	24	40	100	24	19 (*S*)

[a] Catalyst prepared in situ from $[Rh_4(CO)_{12}]$, L/Rh = 1.5, catalyst loading 25 ppm, P = 12 bar, CO/H_2 = 1/1. [b] Catalyst prepared in situ from $[Rh(acac)(CO)_2]$, L/Rh = 1.1, catalyst loading 0.1 mol %, P = 10 bar, CO/H_2 = 1/2. [c] CO/H_2 = 1/1. [d] CO/H_2 = 2/1. [e] Rh/L = 0.5.

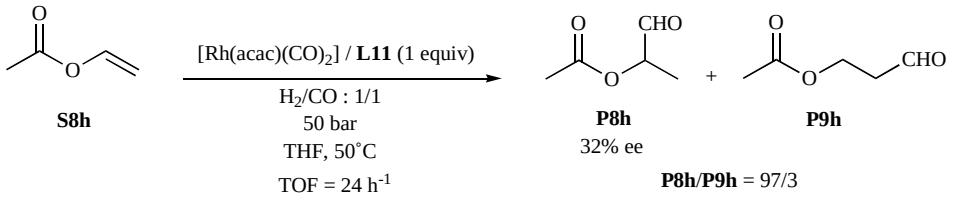

Scheme 32.

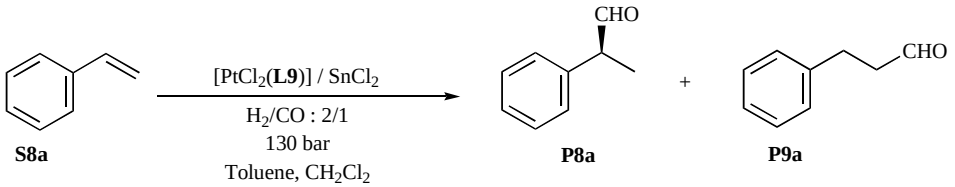

Scheme 33.

Table 20. Hydroformylation of styrene S8a catalyzed by $[PtCl_2L9]$ complex[a]

Entry	Temp. (°C)	Conv. (%)	TOF (h^{-1})	P8a/P9a	e.e. (%)
1	50	97	36	1.2	30 (*S*)
2[b]	50	98	38	1.1	30 (*S*)
3	30	54	20	1.1	38 (*S*)
4	20	41	15	1.1	44 (*S*)

[a] Catalyst loading 10 ppm, t = 18h. [b] CO/H_2 = 1/1.

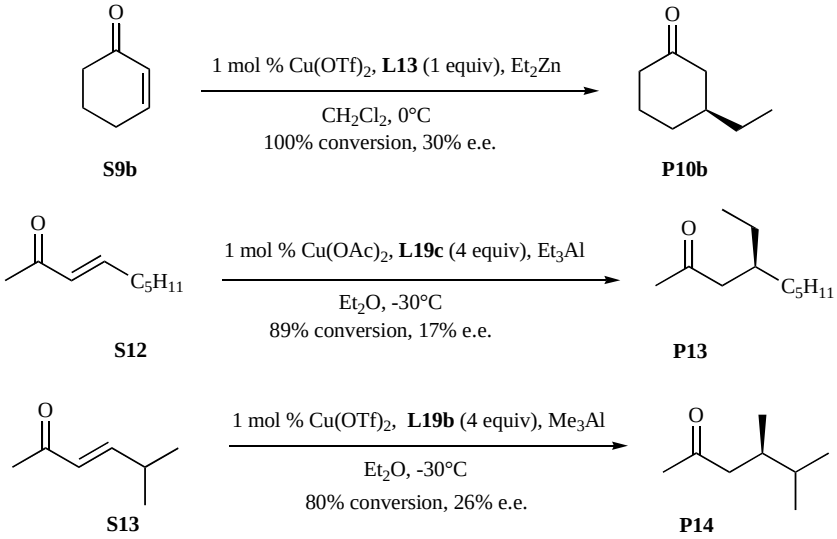

Scheme 34.

study concerning the application of furanoside-based ligands **L19b-c** for the asymmetric 1,4-addition of trialkylaluminium reagents to acyclic enones **S12** and **S13** (Scheme **34**) [37]. Once again, modest results were observed in terms of chiral induction (17 and 26% e.e). It is noteworthy that the high conformational mobility of these substrates makes the design of effective enantioselective systems a real challenge [39].

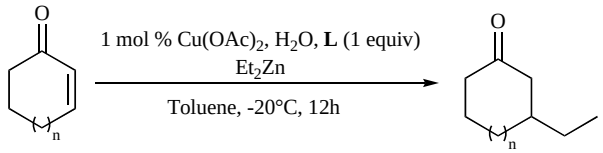

S9a n = 0
S9b n = 1
S9c n = 2
S9d n = 3

P10a n = 0
P10b n = 1
P10c n = 2
P10d n = 3

Scheme 35.

Ligands bearing a tropane scaffold have been investigated in Cu-mediated 1,4-additions to cyclic and acyclic enones (Schemes **35** and **36**, Tables **21** and **22**) [38]. A very pronounced matched/mismatched effect was observed with ligands **L20a-d** for the conjugated addition of diethylzinc to cyclopentenone **S9a** (Table **21**, entries 1-4). The (*S*,*S*)-diastereomer **L20a** and the (*R*,*R*)-diastereomer **L20c** turned out to be the matched ligands. As a general trend, interesting enantioselectivities ranging from 73 to 91% e.e. were obtained with these two ligands for cyclic enones **S9a-d**.

Table 21. Cu-catalyzed conjugate 1,4-addition of diethylzinc to cyclic enones S9a-d

Entry	Substrate	L	Yield (%)	e.e. (%)
1	**S9a**	**L20a**	46	87 (*S*)
2	**S9a**	**L20b**	81	5 (R)
3	**S9a**	**L20c**	55	81 (*S*)
4	**S9a**	**L20d**	70	1 (*R*)
5	**S9b**	**L20a**	99	90 (*S*)
6	**S9b**	**L20c**	98	91 (*S*)
7	**S9c**	**L20a**	70	81 (*S*)
8	**S9c**	**L20c**	79	73 (*S*)
9	**S9d**	**L20a**	89	79 (*S*)
10	**S9d**	**L20c**	83	83 (*S*)

These studies were extended to acyclic substrates. While modest enantioselectivities could be reached with aliphatic substrate **S14** by using ligands **L20a** and **L20d** (Table **22**, entries 1-2), better, albeit only fairly good, results were obtained with aromatic-containing analogues **S15-19**. Moreover, electron-rich groups substituted enones improved the performance of ligand **L20a** (Table **22**, entries 3, 7 and 9) allowing a rise to 59% e.e.

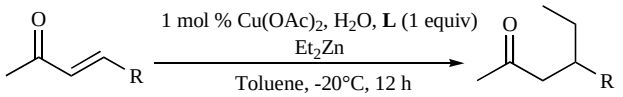

S14 R = *n*-Bu
S15 R = Ph
S16 R = 2-thienyl
S17 R = 2-furyl
S18 R = 4-MeOC$_6$H$_4$
S19 R = 4-ClC$_6$H$_4$

P15 R = *n*-Bu
P16 R = Ph
P17 R = 2-thienyl
P18 R = 2-furyl
P19 R = 4-MeOC$_6$H$_4$
P20 R = 4-ClC$_6$H$_4$

Scheme 36.

2.2.3.4. Allylic Substitution Reactions

Several studies dealing with allylic substitution reactions catalyzed by palladium phosphoramidite-phosphite complexes have been reported. Diéguez and co-workers used their sugar-based ligands for the Pd-catalyzed allylic alkylation of disubstituted linear substrates **S20a-c** (Scheme **37**, Table **23**) [35, 36b]. Pd/**L19a-c** based catalysts proved to be efficient and afforded **P21a** with good ee values (Table **23**, entries 1-3). **L19a-c** behaved quite similarly with each substrate and the only best result is given for **S20b-c** (Table **23**, entries 12 and 13). On the other hand, the screening of ligands **L13-18** highlighted that the substituents of the

Table 22. Cu-catalyzed conjugate 1,4-addition of diethylzinc to acyclic enones S14-19

Entry	Substrate	L	Yield (%)	e.e. (%)
1	**S14**	**L20a**	96	18 (*R*)
2	**S14**	**L20d**	67	17 (*R*)
3	**S15**	**L20a**	46	36 (*R*)
4	**S15**	**L20b**	87	48 (*S*)
5	**S16**	**L20b**	98	56 (n.d.)
6	**S16**	**L20d**	96	67 (n.d.)
7	**S17**	**L20a**	32	56 (n.d.)
8	**S17**	**L20c**	97	24 (n.d.)
9	**S18**	**L20a**	54	59 (n.d.)
10	**S18**	**L20c**	84	39 (n.d.)
11	**S19**	**L20b**	59	53 (n.d.)

n.d.: not determined

biphenyl moieties, the configuration of carbon atom C-3 and the configuration of binaphtyl groups influenced the catalytic performance in terms of activity and chiral induction (Table **23**, entries 4-11). In summary, the best enantioselectivity (e.e. up to 98%) was obtained with **L17b** (Table **23**, entry 9). It should be noted that a strong matched/mismatched effect was also observed with this catalytic system (Table **23**, entries 8-9 and 10-11).

The potential of these ligands was then evaluated for the alkylation of disubstituted cyclic substrates **S21a-b** (Scheme 38, Table **24**) [35,36b]. The results of the study of ligands **L19a-c** indicate that substituents at *para* positions of the biphenyl moieties are required for better asymmetric inductions (Table **24**, entry 3 *vs*. 1 and 2; entry 6 *vs*. 4 and 5). Remarkably, despite a lower reactivity, higher enantioselectivities were obtained with seven-membered ring substrate **S21b** than with six-membered ring substrate **S21a**. On the other hand, the use of ligand **L15** afforded interesting results for the allylic alkylation of **S21a** and **S21b** reaching 85 and 91% e.e. respectively (Table **24**, entries 7 and 8).

Finally, the allylic substitution of monosubstituted linear substrates was also examined (Scheme 39, Table **25**) [35,36b]. Besides the enantioselectivity, the control of the regioselectivity still remains a challenge for this transformation. As illustrated in Table **25**, only ligand **L18a** allowed for both interesting regio- and enantioselectivities (Table **25**, entry 4).

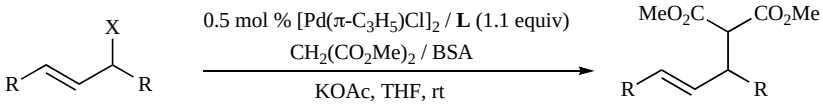

S20a R = Ph, X = OAc
S20b R = ^{i}Pr, X = OCO_2Et
S20c R = Me, X = OAc

P21a R = Ph
P21b R = ^{i}Pr
P21c R = Me

Scheme 37.

Table 23. Pd-catalyzed allylic alkylation of disubstituted linear substrates S20a-c

Entry	Substrate	L	Time (h)	Conv. (%)	e.e. (%)
1	**S20a**	**L19a**	0.5	100	84 (*R*)
2	**S20a**	**L19b**	0.5	100	76 (*R*)
3	**S20a**	**L19c**	0.5	100	81 (*R*)
4[a]	**S20a**	**L13**	0.25	88	62 (*S*)
5[a]	**S20a**	**L14**	0.25	100	59 (*S*)
6[a]	**S20a**	**L15**	0.25	64	55 (*S*)
7[a]	**S20a**	**L16**	0.25	83	52 (*S*)
8[a]	**S20a**	**L17a**	0.5	71	6 (*S*)
9[a]	**S20a**	**L17b**	0.5	96	98 (*S*)
10[a]	**S20a**	**L18a**	2	12	80 (*S*)
11[a]	**S20a**	**L18b**	2	15	12 (*S*)
12	**S20b**	**L19a**	18	100	89 (*S*)
13	**S20c**	**L19c**	0.5	100	61 (*R*)
14[a]	**S20c**	**L18b**	4	82	84 (*S*)

[a] CH_2Cl_2 was used as solvent.

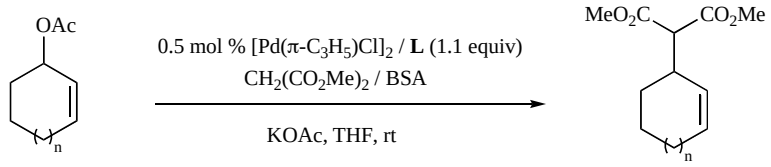

S21a n = 1
S21b n = 2

P22a n = 1
P22b n = 2

Scheme 38.

Table 24. Pd-catalyzed allylic alkylation of disubstituted cyclic substrates S21a-b

Entry	Substrate	L	Time (h)	Conv. (%)	e.e. (%)
1	**S21a**	**L19a**	2	100	48 (*S*)
2	**S21a**	**L19b**	2	100	46 (*S*)
3	**S21a**	**L19c**	2	100	22 (*S*)
4	**S21b**	**L19a**	2	17	82 (*S*)
5	**S21b**	**L19b**	2	16	81 (*S*)
6	**S21b**	**L19c**	2	12	42 (*S*)
7[a]	**S21a**	**L15**	2	100	85 (*S*)
8[a]	**S21b**	**L15**	6	52	91 (*S*)

[a] CH_2Cl_2 was used as solvent.

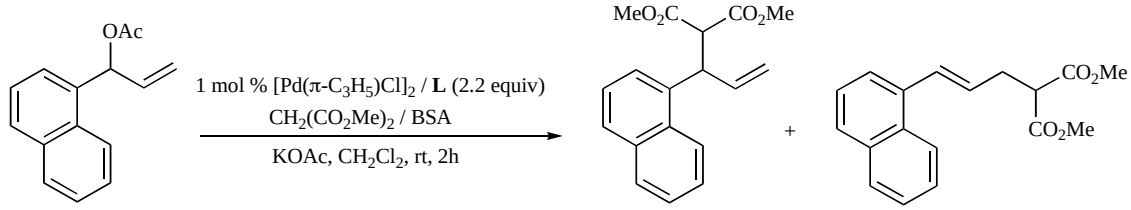

S22 **P23** **P24**

Scheme 39.

Table 25. Pd-catalyzed allylic alkylation of non-symmetric acyclic substrate S22

Entry	L	Conv. (%)	P23/P24	e.e. (%)
1	**L19a**	100	20/80	72 (*S*)
2	**L19b**	100	25/75	28 (*S*)
3	**L19c**	100	40/60	41 (*S*)
4	**L18a**	73	70/30	90 (*S*)

2.3. Phosphoramidite-Phosphinite Ligands

2.3.1. Overview

Following the screening of potential chelating groups, the synthesis of new phosphoramidite-phosphinite ligands was undertaken. This section will deal with the synthesis of these ligands and the applications in which they were involved.

2.3.2. Synthesis of Phosphoramidite-Phosphinite Ligands

The first synthesis of a phosphoramidite-phosphinite ligand was published by the group of Agbossou in 2000 (Scheme **40**) [29]. Starting from ephedrine **25**, they first introduced the phosphinite moiety by reacting PPh_2NMe_2 with the previous cited amino alcohol. Then, via a classical procedure of phosphoramidite synthesis, they succeeded in preparing ligands **L21a-d** in good to moderate yields.

Few years later, Cesarotti and co-workers reported the synthesis of ligands **L22** and **L23** (Scheme **41**) [31,40]. The chiral amino alcohols **37** and **38** were successively treated with sodium hydride and chlorodiphenylphosphine to form the corresponding amino-phosphinites derivatives. Then, ligands **L22** and **L23** were synthesized following the classical procedure previously described.

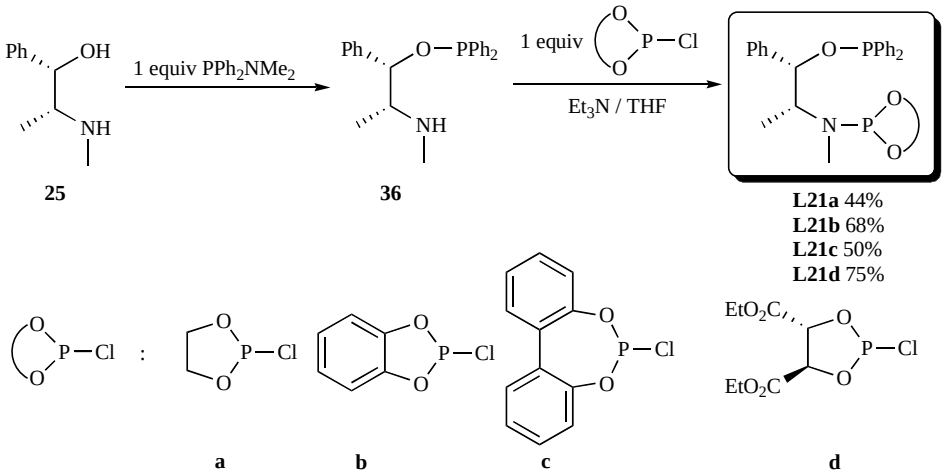

Scheme 40.

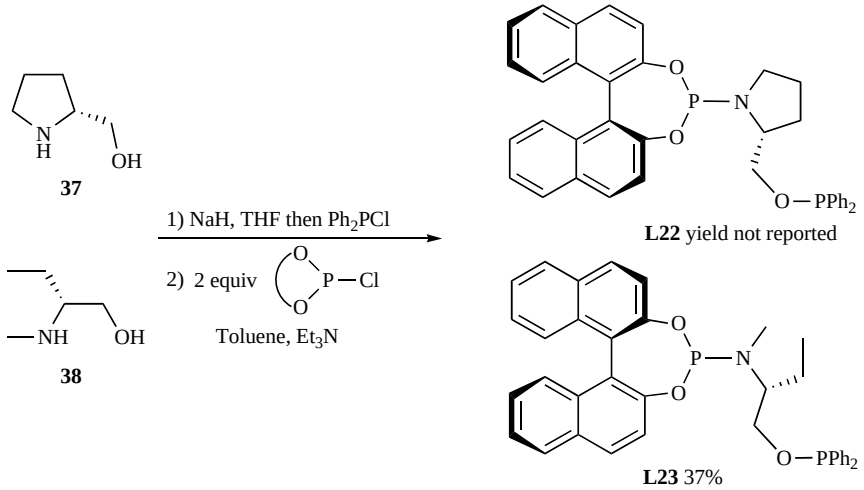

Scheme 41.

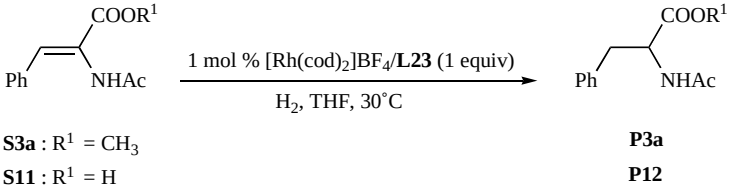

Scheme 42.

2.3.3. Evaluation of Phosphoramidite-Phosphinite Ligands In Asymmetric Catalysis

Only two asymmetric processes have been investigated with these ligands: the hydrogenation and the hydroformylation of alkenes.

2.3.3.1. Hydrogenation of Carbon-Carbon Double Bonds

The rhodium-catalyzed hydrogenation of β-(acylamino) acrylates **S3a** and **S11** using phosphoramidite-phosphinite **L23** ligand was reported by Cesarotti and co-workers (Scheme **42**, Table **26**) [31]. A slight matched/mismatched effect was detected by comparing **L23** and its (*S*)-BINOL-containing diastereomer (Table **26**, entry 1 *vs.* 3 and entry 2 *vs.* 4), but the enantioselectivities measured were relatively low in both cases (7 to 44% e.e.).

2.3.3.2. Hydroformylation

The use of ligands **L21a-d** in the asymmetric rhodium-catalyzed hydroformylation of styrene **S8a** has been described by the group of Agbossou (Scheme **43**, Table **27**) [29]. As a general trend, good activities and selectivities in favour of the branched aldehyde **P8a** have been observed. Unfortunately, only poor enantioselectivities were obtained for these reactions (5 to 20% e.e.).

Asymmetric rhodium-catalyzed hydroformylations of additional olefins using phosphoramidite-phosphinite ligands have been investigated by Cesarotti. First, the use of vinylacetate **S8h** as substrate either with ligand **L22** or with **L23** afforded compound **P8h** with good selectivities but very low e.e. values (Scheme **44**) [31]. In this case, better results were

Table 26. Hydrogenation of β-(acylamino)acrylates catalyzed by Rhodium/ phosphoramidite-phosphinite L23 complex

Entry	Substrate	Pressure (bar)	Time (min)	Conv. (%)	e.e. (%)
1	**S3a**	100	3	100	44 (*S*)
2	**S11**	1	210	100	24 (*S*)
3[a]	**S3a**	10	40	100	17 (*R*)
4[a]	**S11**	1	300	100	7 (*R*)

[a] Obtained with (*S*)-BINOL-containing diastereomer of **L23**.

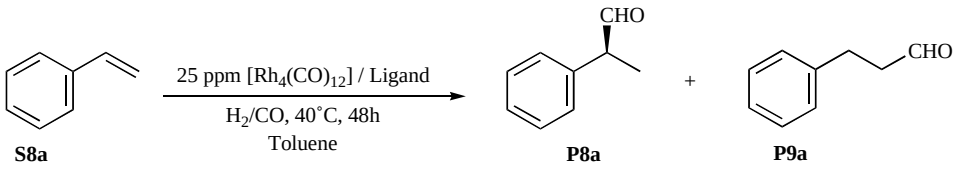

Scheme 43.

Table 27. Hydroformylation of styrene catalyzed by rhodium / phosphoramidite-phosphinite L21a-d complexes[a]

Entry	Ligand	Conv. (%)	P8a/P9a	e.e. (%)
1	**L21a**	66	11	5 (*R*)
2	**L21b**	71	14	5 (*R*)
3	**L21c**	86	9	15 (*R*)
4	**L21d**	88	9	20 (*S*)

[a] L/Rh = 1.5, P = 12 bar, CO/H_2 = 1/1.

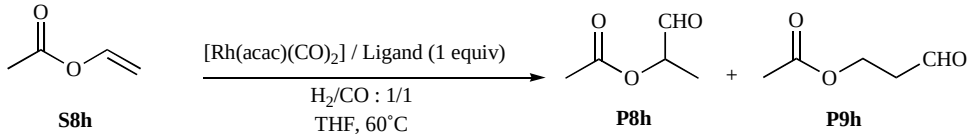

L22, 70 bar, TOF = 60 h^{-1}, 12% ee, **P8h**/**P9h** = 95/5
L23, 30 bar, TOF = 96 h^{-1}, 19% ee, **P8h**/**P9h** = 99/1

Scheme 44.

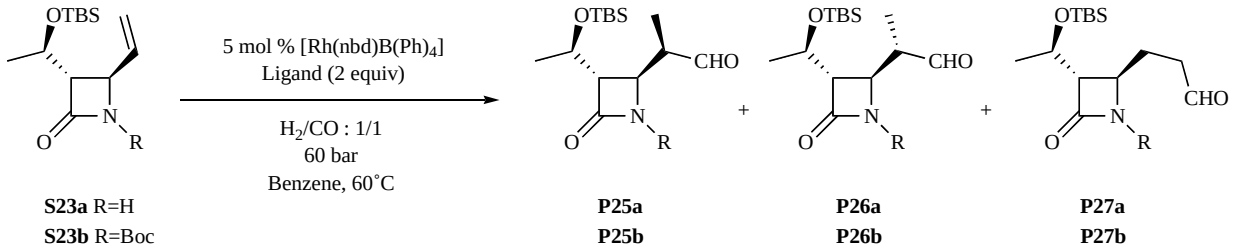

Scheme 45.

obtained with ligand **L11**, phosphoramidite-phosphite analogue of **L22** (see Scheme **32**).

On the other hand, the hydroformylation of azetidinones **S23a-b** catalyzed by rhodium/ phosphoramidite-phosphinite **L23** system was studied in the synthesis of 1-methylcarbapenem precursors (Scheme **45**, Table **28**) [40]. Modest regio- and diastereoselectivities were reached in this process. In the case of substrate **S23b,** a strong difference of activity was detected between the two diastereomers of **L23** (Table **28**, entries 2 and 3). The chirality of the major diastereoisomer was controlled by the configuration of the BINOL moiety.

2.4. Phosphoramidite-Thioether Ligands

2.4.1. Overview

The first and to date the only phosphoramidite-thioether ligands have been reported by Crévisy and Mauduit in 2006 [23]. These ligands are based on a BINOL skeleton and bear a chelating arm containing a thioether moiety on the amine

Table 28. Hydroformylation of 4-vinyl β-lactams S23 catalyzed by rhodium/ phosphoramidite-phosphinite L23 complex

Entry	Substrate	Time (h)	Conv. (%)[a]	e.e.(%)
1	**S23a**	60	68	22 (*S*)
2	**S23b**	17	24	24 (*S*)
3[b]	**S23b**	78	12	22 (*R*)

[a] Conversion measured for **P25**+**P26**. [b] Obtained with (*S*)-BINOL-containing analogue of **L23**.

part. In this section, both synthesis and applications of these compounds will be discussed.

2.4.2. Synthesis of Phosphoramidite-Thioether Ligands

These bidentate phosphoramidite ligands were synthesized from different commercially available β-amino alcohols for **L24-28** and from *o*-methylthioaniline for **L29** according the synthesis illustrated in Scheme **46** [23]. Following the procedure described by Feringa [4a], amines **39** were first reacted with PCl_3 in the presence of Et_3N before the addition of a BINOL solution. Thus, the corresponding phosphoramidites **L24-27**, bearing various R^1 and R^2 groups, were obtained in good to moderate yields. A similar route was used for the synthesis of **L28** and **L29** starting from amines **40** and **41**. It is noteworthy that the steric hindrance and the rigidity of the chelating arm could be modulated by using different secondary amines **39-41** for the ligand synthesis.

2.4.3. Evaluation of Phosphoramidite-Thioether Ligands in Asymmetric Catalysis

To date, only the asymmetric copper-catalyzed conjugate addition has been investigated with these bidentate phosphoramidite-thioether ligands.

2.4.3.1. Cu-Catalyzed Conjugate Addition on Enones

Ligands **L24-29** have been evaluated in the 1,4-addition of diethylzinc to cyclic and acyclic enones **S9b** and **S13** (Scheme **47**, Table **29**) [23]. A matched/mismatched effect was observed by comparing **L25a** and **L25b** in one hand, and then **L26a** and **L26b** on the other hand (Table **29**, entries 1, 2, 4 and 5). The influence of R^2 group on the chiral center was also investigated, highlighting that a bulky substituents such as *t*-butyl led to lower activities and selectivities. How-

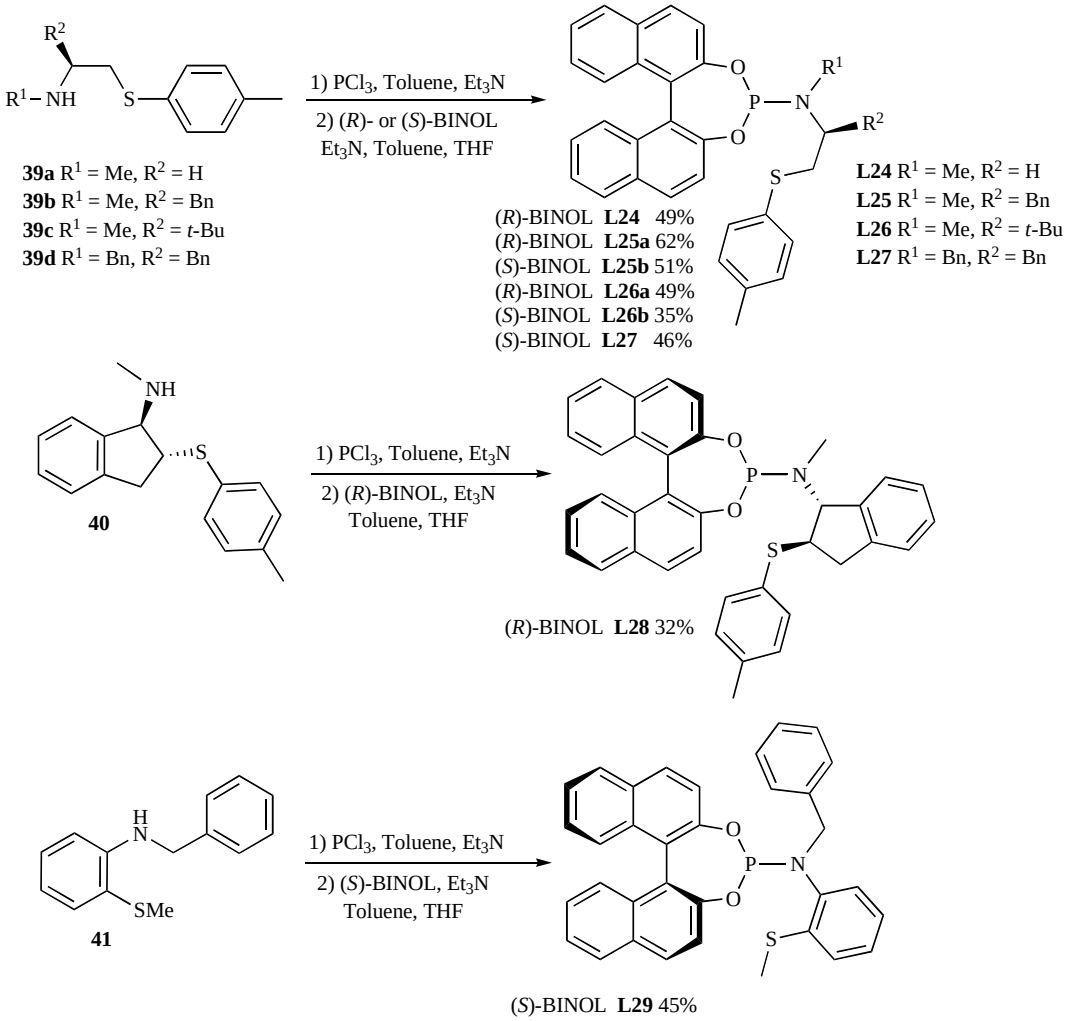

Scheme 46.

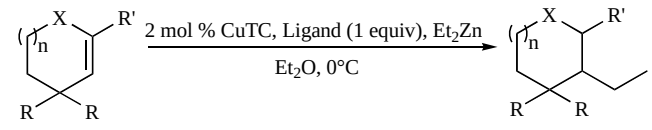

S9b	n = 1, X = C=O, R = H, R' = H	**P10b**
S24	n = 1, X = C=O, R = Me, R' = H	**P29**
S9c	n = 2, X = C=O, R = H, R' = H	**p10c**
S25	n = 1, X = CH_2, R = H, R' = NO_2	**P30**

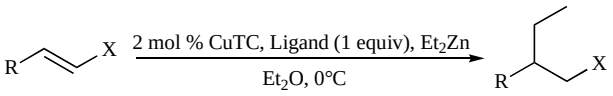

S15	X = $COCH_3$, R = Ph	**P16**
S12	X = $COCH_3$, R = C_5H_{11}	**P13**
S13	X = $COCH_3$, R = *i*-Pr	**P28**
S26	X = NO_2, R = Ph	**P31**

Scheme 47.

ever, the absence of a stereogenic center in that position led to a strong decrease of the enantioselectivity for acyclic enone **S9b** (Table **29**, entry 10) whereas a slighter effect was noticed with a cyclic substrate (Table **29**, entry 3). The introduction of a benzyl group on R^1 position did not improve the results (Table **29**, entry 6). Likewise, more rigid ligands such as **L28** and **L29** were not found very efficient for this application (Table **29**, entries 7 and 8). In summary, the best results were reached with **L25b** for both cyclic and acyclic enones **S9b** and **S13** (Table **29**, entries 1 and 9).

The scope of this catalytic system was extended using **L25b** (Scheme **47**, Table **30**). The best enantioselectivity was reached with sterically hindered 4,4-dimethylcyclohexenone **S24** (Table **30**, entries 1 and 2). Of note, a temperature decrease did not allow for significative improvement in term of chiral induction on this compound, but affected notably the catalytic activity. A high reactivity but a moderate enantioselectivity were found with the cycloheptenone **S9c** (Table **30**, entry 3). The study of acyclic substrates **S12**, **S13** and **S15** revealed that good TON could be obtained (Table **30**, entries 5, 6 and 7). Nevertheless, interesting enantiomeric excesses were only reached for **S12** and **S13** (Table **30**, entries 6 and 7). Finally, modest results in terms of selectivity were observed with cyclic and acyclic nitroalkenes **S25** and **S26** in spite of the good catalytic activity (Table **30**, entries 4 and 8).

2.5. Miscellaneous

2.5.1. Overview

Besides the main families of hybrid phosphoramidite presented above, various chelating groups have been connected to phosphoramidites to form hybride bidentate ligands. Notably, two families of P,N ligands were reported in 2000 and 2003 [41, 42]. In both cases, the *N*-chelating group is carried by the non-chiral amino moiety of the phosphoramidite group. Both ligands are made of a BINOL moiety and the *N*-chelating group was obtained from a 2-aminopyridine in **L30a-b** or from 8-aminoquinoline in **L31** (Scheme **48**). The authors also reported a polymer-supported version of **L31**. A soluble styrene-based copolymer was chosen as the support (**L32**, Scheme **48**). Later, Douthwaite reported his investigations dealing with the use of phosphoramidite-chiral NHC bidentate ligands **L33a-c** in the Pd-catalyzed allylic substitution reaction (Scheme **48**) [43a]. He had previously obtained low rates when he used the corresponding di-NHC and NHC-imine ligands in this reaction. He anticipated that the replacement of either one NHC or the imino chelating group by a phosphine could increase the rate. Very recently, phosphoramidite-chiral oxazoline bidentate ligands **L34a-f** were obtained by Guiry [44]. Again, the oxazoline coordinating site is carried by the amino unit of the phosphoramidite. Is is interesting to note that **L34a-f** are made of a TADDOL moiety instead of the usually used BINOL framework (Scheme **48**).

2.5.2. Synthesis of Ligands L30-L34

L30 and **L31** were readily prepared in one step from (*S*)-1,1'-bi-2-naphtyl chlorophosphite **44** and commercially available 2-aminopyridine **42a** or **42b** and 8-aminoquinoline

Table 29. Cu-catalyzed conjugate 1,4-addition of diethylzinc to cyclic and acyclic enones S9b and S13

Entry	Substrate	L	Time (h)	Conv. (%)	e.e. (%)
1	**S9b**	**L25b**	3	>99	72 (*S*)
2	**S9b**	**L25a**	4	96	56 (*R*)
3	**S9b**	**L24**	3	93	65 (*R*)
4	**S9b**	**L26a**	2.5	>99	30 (*R*)
5	**S9b**	**L26b**	6	72	56 (*S*)
6	**S9b**	**L27**	4	54	66 (*S*)
7	**S9b**	**L28**	3	>99	47 (*R*)
8	**S9b**	**L29**	3	>99	0
9	**S13**	**L25b**	3	93	63 (*R*)
10	**S13**	**L24**	5	80	33 (*S*)

Table 30. Cu-catalyzed conjugate 1,4-addition of diethylzinc to cyclic and acyclic enones with ligand L25b

Entry	Substrate	Time (h)	Conv. (%)	e.e. (%)
1	**S24**	6	60	78
2[a]	**S24**	6	12	80
3	**S9c**	6	96	64
4	**S25**	6	82	16
5	**S15**	1	>99	17
6	**S12**	1	96	52
7	**S13**	3.5	93	63
8	**S26**	4	>99	6

[a] Reaction performed at -30ºC.

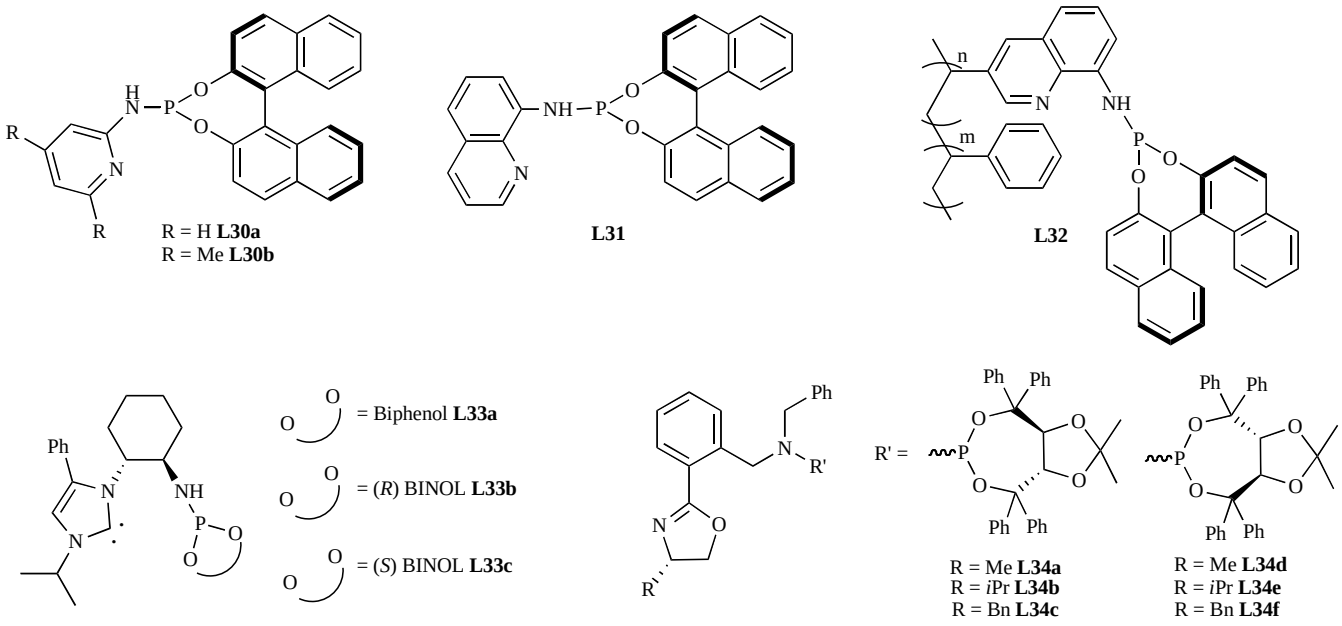

Scheme 48.

43 respectively (Scheme **49**) [41-42]. Polymer-supported **L32** was obtained by co-polymerisation of styrene with the analogue of **L31** bearing a vinyl group at the 3-position of the quinoline group, **46**. The later was in turn synthesized, in a 22% overall yield, from 3-bromoquinoline **45** following a classical four step procedure (Scheme **49**) [42].

Ligands **L33a-c** were generated in situ from corresponding imidazolium-phosphoramidites **51a-c** (Scheme **50**) [43]. Compounds **51a-c** were prepared from (1*R*,2*R*)-diaminocyclohexane **47** in a rather long but efficient five-step procedure (45-52% overall yield). Diamine **47** was converted to diimine **48** which was then submitted to a 1,3-cycloaddition reaction with TosMIC to give imidazole-imine **49**. The imine group was hydrolyzed affording the corresponding amine which was then converted to phosphoramidites **50a-c** following classical conditions. The imidazole-phosphoramidites **50a-c** were then treated with *i*PrI to afford imidazolium-phosphoramidites **51a-c**.

Ligands **L34a-f** were obtained in a three-step procedure from commercially available aminoalcohols **52a-c** (Scheme **51**) [44]. $ZnCl_2$- or $ZnBr_2$-catalyzed condensation of aminoalcohols **52a-c** and α-bromo-*o*-tolunitrile **53** afforded oxazolines **54a-c** which were then subjected to a nucleophilic substitution with benzylamine to give amines **55a-c**. Amines **55** were converted to phosphoramidite-oxazolines **L34a-f** following a classical procedure employed for the formation of phosphoramidite groups [26].

2.5.3. Evaluation of Ligands L30-L34 in Asymmetric Catalysis

The efficiency of Ligands **L30**, **L33** and **L34** was evaluated in the palladium-catalyzed asymmetric allylic substitution reaction. The rhodium complexes of **L31** and **L32** were tested in the Rh-catalyzed hydrogenation of alkenes. The efficiency of **L33** was also investigated in the iridium-catalyzed transfer hydrogenation reaction. Ligands **L34** were

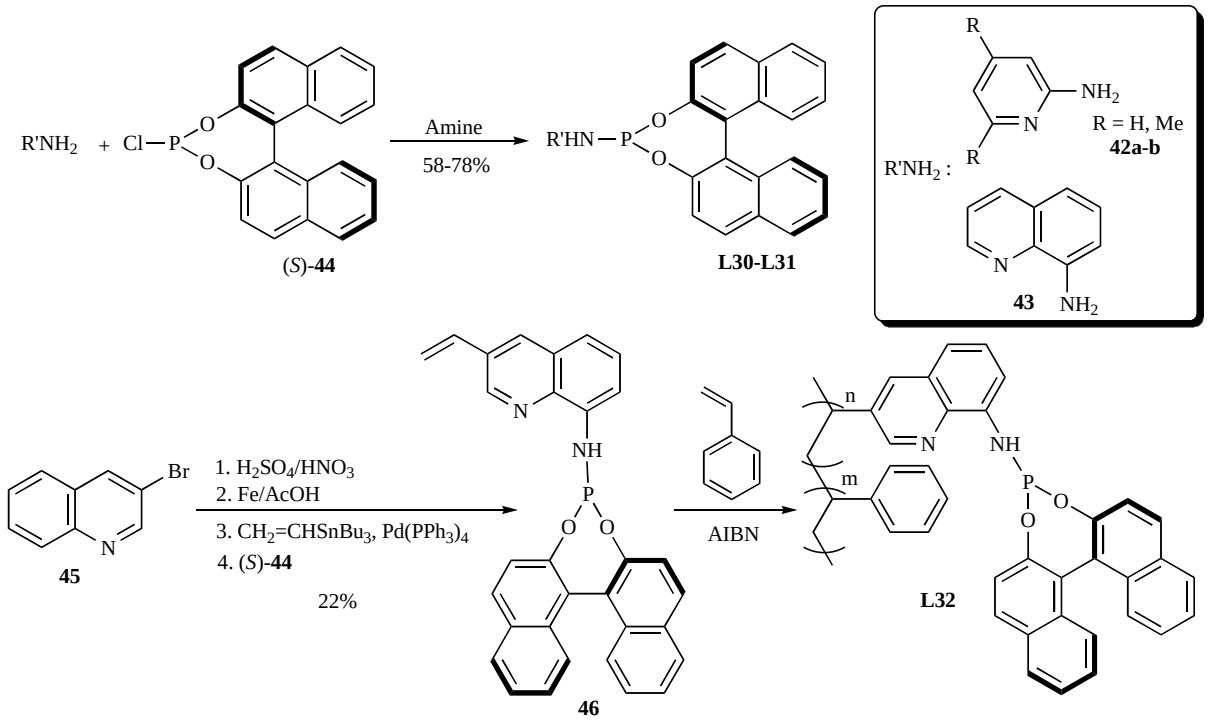

Scheme 49.

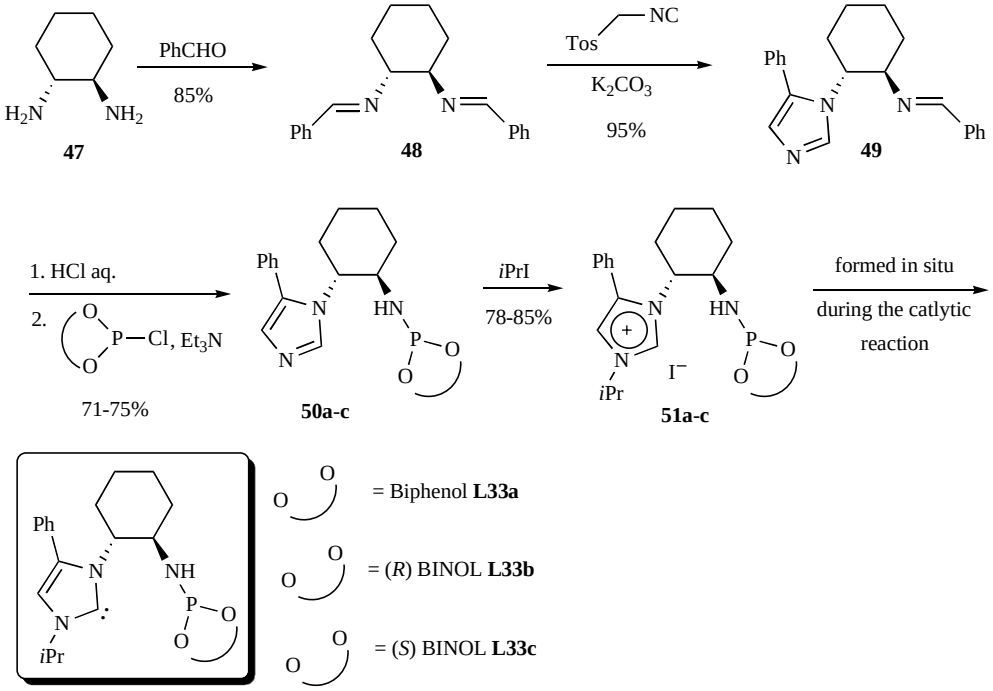

Scheme 50.

also examined in the asymmetric Suzuki-Miyaura coupling reaction.

2.5.3.1. Hydrogenation of Carbon-Carbon Double Bonds

The **L31** rhodium complex, [Rh(**L31**)(cod)]BF_4 **56,** was prepared, isolated and then tested in the hydrogenation of dimethylitaconate **S1a**, dehydroaminoesters **S2** and **S3a** and dehydraminoacids S**27** and **S11** (Scheme **52**) [42]. Reactions were performed under low pressure of hydrogen (1 bar) but rather high Rh loading (5 mol %). Full conversions were achieved after 4h or 20h at room temperature, except when dehydroaminoacids **S27** and **S11** were engaged in the reaction. The hydrogenated products were isolated in only modest to good enantioselectivities (63-95% ee), **S1a** affording the best ee value. It is interesting to compare the aforementioned results with those obtained with the polymer-supported analogue **L32** [42]. The supported complex [Rh/**L32**] was prepared, isolated and tested in the hydrogena-

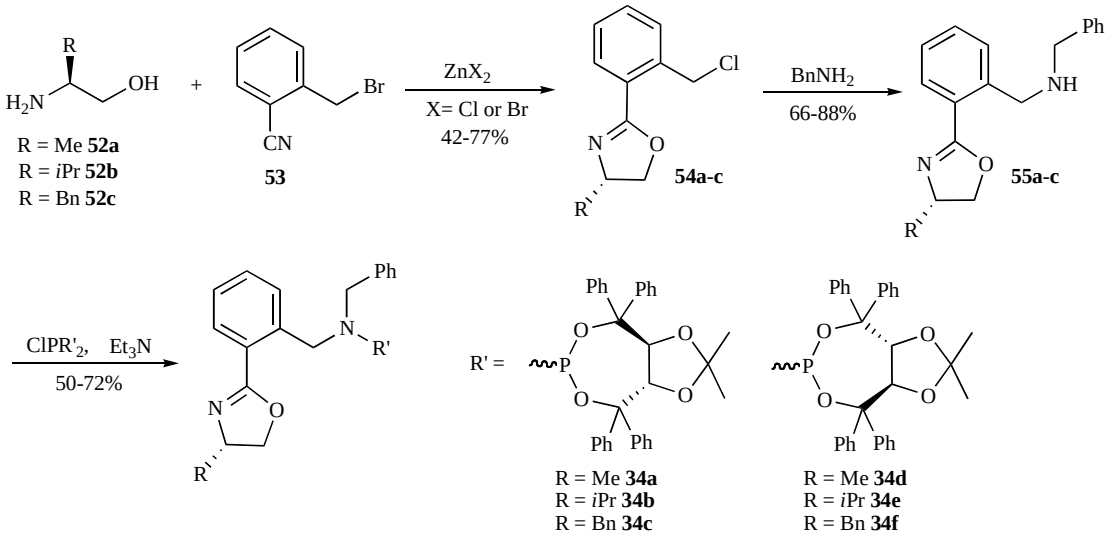

R = Me **52a**
R = *i*Pr **52b**
R = Bn **52c**

53

54a-c

55a-c

R = Me **34a**
R = *i*Pr **34b**
R = Bn **34c**

R = Me **34d**
R = *i*Pr **34e**
R = Bn **34f**

Scheme 51.

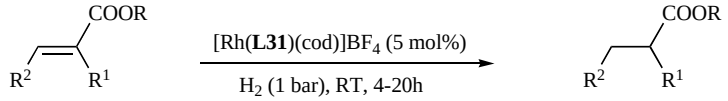

S1a : R = Me, R^1 = CH_2COOMe, R^2 = H
S2 : R = Me, R^1 = NHAc, R^2 = H
S3a : R = Me, R^1 = NHAc, R^2 = Ph
S27 : R = H, R^1 = NHAc, R^2 = H
S11 : R = H, R^1 = NHAc, R^2 = Ph

P1a 95% ee (*S*), 100% conv.
P2 84% ee (*R*), 100% conv.
P3a 78% ee (*R*), 100% conv.
P32 63% ee (*R*), 49% conv.
P12 75% ee (*R*), 98% conv.

Scheme 52.

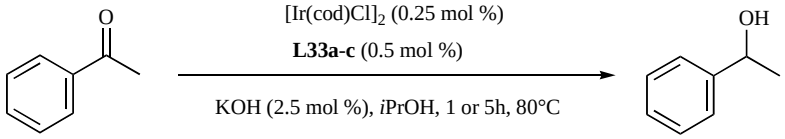

S7a

84-87% yield, 15-37% ee after 1h
94-96% yield, 12-34% ee after 5h

P7a

Scheme 53.

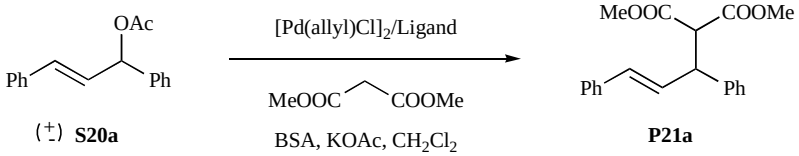

(±) **S20a**

P21a

Scheme 54.

tion reaction of **S1a**, **S2**, **S3a**, **S27** and **S11**. Under the same reaction conditions as those used previously with complex **56**, it was observed that both the conversions (23-100%) and the enantioselectivities (49-65% ee) were lower than those obtained with the non-supported complex **56**.

2.5.3.2. Iridium-Catalyzed Transfer Hydrogenation of Carbon-Oxygen Double Bond

NHC-phosphoramidites **L33a-c** were tested in the iridium-catalyzed transfer hydrogenation of acetophenone **S7a** (Scheme **53**) [43a]. The reactions were conducted for 1h and 5h in the presence of 0.25 mol % catalyst at 80°C and afforded alcohol **P7a** in good yield (84-87% after 1h reaction) albeit with a low enantioselectivity (15-37% ee after 1h reaction).

2.5.3.3. Pd-Catalyzed Allylic Substitution Reaction

The palladium-catalyzed allylic substitution reaction of (*E*)-1,3-diphenylprop-2-en-1-yl acetate **S20a** and dimethylmalonate anion using P,N-ligands **L30a-b** [41], NHC-phosphoramidites **L33a-c** [43a] and phosphoramidite-oxazoline ligands **L34a-f** [44] was investigated (Scheme **54**). For a better comparison of the ligand efficiencies, the results are gathered in Table **31**. Amino-phosphoramidite ligands **L30a-b** and NHC-phosphoramidites **L33a-c** gave **P21a** in good yields (86-97%, entries 1-5) but with a low enantioselectivity (17-42% ee, entries 1-5). Better, but only rather good ee values, were obtained by using phosphoramidite-oxazoline ligands **L34a-f** [44]. Among the analogue series **L34a-f**, the matched ligands **L34d-f** afforded the highest

Table 31. Pd-catalyzed allylic substitution of (*E*)-1,3-diphenylprop-2-en-1-yl acetate S20a and dimethylmalonate

Entry	Ligand	Pd/Ligand (mol %)	Temp. (°C)	Time (h)	Yield (%)	e.e (%)
1	**L30a**	0.5/1.25	n.c.	16	93	37 (*S*)
2	**L30b**	0.5/1.25	n.c.	16	90	33 (*S*)
3	**L33a**	2.5/5.0	25	5	97	17 (*S*)
4	**L33b**	2.5/5.0	25	5	95	11 (*R*)
5	**L33c**	2.5/5.0	25	5	86	42 (*S*)
6	**L34a**	0.5/0.55	20	48	22[a]	64 (*R*)
7	**L34b**	0.5/0.55	20	48	86[a]	73 (*R*)
8	**L34c**	0.5/0.55	20	48	68[a]	78 (*R*)
9	**L34d**	0.5/0.55	20	48	71[a]	87 (*S*)
10	**L34e**	0.5/0.55	20	48	46[a]	81 (*S*)
11	**L34f**	0.5/0.55	20	48	41[a]	88 (*S*)

[a] Conversion is given

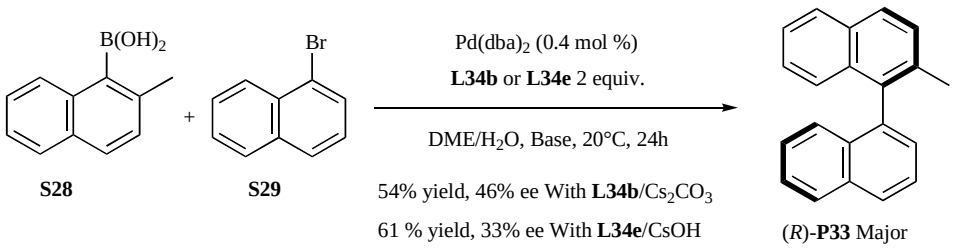

Scheme 55.

enantioselectivities (81-88% ee, entries 9-11), nevertheless the unmatched ligand **L34b** gave the most active catalyst (86% conversion after 48h at 0.5 mol % catalyst loading, entry 7). It can be noticed that the configuration of the TADDOL moiety plays the main role in the control of the absolute configuration in **P21a**.

2.5.3.4. Pd-catalyzed Asymmetric Suzuki-Miyaura Coupling Reaction

Guiry applied the phosphoramidite-oxazoline ligands **L34b** and **L34e** in the Pd-catalyzed Suzuki-Miyaura coupling between 2-methylnaphtylboronic acid **S28** and 1-bromonaphtalene **S29** (Scheme **55**). Many bases were tested and it was observed that both the conversion and the ee value were dependant upon the couple ligand/base. With the most efficient ligand/base couples, 2-methyl-1,1'-binaphtyl **P33** was isolated in both moderate yield and enantioselectivity. Contrary to what was observed in the allylic substitution reaction (cf. 2.5.3.3) the authors noted that, in this reaction, the configuration of the oxazoline moiety controls the chirality of the coupling product.

3. CONCLUSION

Since 2000, various hybrid bidentate phosphoramidite ligands have been synthesized and applied to asymmetric catalysis. Some are valuable ligands since they can be obtained through short and efficient synthetic routes and they afford metal complexes that exhibit both high activities and enantioselectivites. Particularly noteworthy are phosphoramidite-phosphine ligands **L4c**, **L4i**, **L4f**, **L5d**, **L5e** and **L5h**. For instance, **L5h** gave very interesting results in the hydrogenation reaction of enol ester phosphonates. The worth of **L5e** has to be underlined, although the synthetic process for its synthesis is fairly efficient. Indeed, this ligand led to outstanding results in the hydroformylation of styrenes. Phosphoramidite-phosphite ligands proved to be less efficient. Nevertheless, very encouraging results were obtained with **L13** and **L17b**, in the hydrogenation of C-C double bonds and in the allylic substitution reaction respectively. On the contrary, the few reported phosphoramidite-phosphite, phosphoramidite-thioether, phosphoramidite-NHC, phosphoramidite-amine and phosphoramidite-oxazoline ligands did not provide high enantioselectivities in the reactions in which they have been applied.

It is hoped that this review has highlighted the opportunities which are offered by this type of recently described ligands and so that new researches will be stimulated in this area.

REFERENCES

[1] (a) Jacobsen, E. N.; Pfaltz, A.; Yamamoto, H. Eds., *Comprehensive Asymmetric Catalysis I-III* (Springer, Berlin, **1999**. (b) Tang, W.; Zhang, X. *Chem. Rev.* **2003**, *103*, 3029. (c) Blaser, H.-U.; Malan, C.; Pugin, B.; Spindler, F.; Steiner, H.; Studer, M. *Adv. Synth. Catal.* **2003**, *345*, 103.

[2] Togni, A.; Breutel, C.; Schnyder, A.; Spindler, F.; Landert, H.; Tijani, A. *J. Am. Chem. Soc.* **1994**, *116*, 4062.

[3] Blaser, H.-U.; Pugin, B.; Spindler, F. *J. Mol. Catal. A: Chem.* **2005**, *231*, 1.
[4] Selected references: (a) de Vries, A. H. M.; Meetsma, A.; Feringa B. L. *Angew. Chem. Int. Ed.* **1996**, *35*, 2374. (b) van den Berg, M.; Minnaard, A. J.; Schudde, E. P.; van Esch, J.; de Vries, A. H. M.; de Vries, J. G.; Feringa, B. L. *J. Am. Chem. Soc.* **2000**, *122*, 11539.
[5] For reviews, see: (a) Jerphagnon, T.; Renaud, J.-L.; Bruneau, C. *Tetrahedron: Asymmetry* **2004**, *15*, 2101. (b) de Vries, J. G.; Lefort, L. *Chem. Eur. J.* **2006**, *12*, 4722 and references cited therein.
[6] Polet, D.; Alexakis, A.; Tissot-Crosset, K.; Corminboeuf, C.; Ditrich, K. *Chem. Eur. J.* **2006**, *12*, 3596 and references cited therein.
[7] Guo, X.-X.; Xie, J.-H.; Hou, G.-H.; Shi, W.-J.; Wang, L.-X.; Zhou, Q.-L. *Tetrahedron: Asymmetry* **2004**, *15*, 2231.
[8] Zhang, A.; Rajanbabu, T. V. *J. Am. Chem. Soc.* **2006**, *128*, 5620 and references cited therein.
[9] Moteki, S. A.; Wu, D.; Chandra, K. L.; Reddy, D. S.; Takacs, J. M. *Org. Lett.* **2006**, *8*, 3097 and references cited therein.
[10] (a) Zhang, W.; Wang, C. J.; Gao, W.; Zhang, X. *Tetrahedron Lett.* **2005**, *46*, 6087. (b) Jagt, R. B. C.; de Vries, J. G.; Feringa, B. L.; Minnaard, A. J. *Org. Lett.* **2005**, *7*, 2433 and references cited therein.
[11] Guiry, P. J.; Saunders, C. P. *Adv. Synth. Catal.* **2004**, *346*, 497.
[12] (a) Francio, G.; Faraone, F.; Leitner, W. *Angew. Chem. Int. Ed.* **2000**, *39*, 1428. (b) Burk, S.; Francio, G.; Leitner, W. *Chem. Commun.* **2005**, 3460.
[13] Wassenaar, J.; Reek, J. N. H. *Dalton Trans.* **2007**, 3750.
[14] Jia, X.; Li, X.; Lam, W. S.; Kok, S. H. L.; Xu, L.; Lu, G.; Yeung, C.-H.; Chan, A. S. C. *Tetrahedron: Asymmetry* **2004**, *15*, 2273.
[15] Hu, X.-P.; Zheng, Z. *Org. Lett.* **2004**, *6*, 3585.
[16] Hu, X.-P.; Zheng, Z. *Org. Lett.* **2005**, *7*, 419.
[17] Zeng, Q.-H.; Hu, X.-P.; Duan, Z.-C.; Liang, X.-M.; Zheng. Z. *Tetrahedron: Asymmetry* **2005**, *16*, 1233.
[18] Huang, J.-D.; Hu, X.-P.; Duan, Z.-C.; Zeng, Q.-H.; Yu, S.-B.; Deng, J.; Wang, D.-Y.; Zheng, Z. *Org. Lett.* **2006**, *8*, 4367.
[19] Yan, Y.; Zhang, X. *J. Am. Chem. Soc.* **2006**, *128*, 7198.
[20] Vallianatou, K. A.; Kostas, I. D.; Holz, J.; Börner, A. *Tetrahedron Lett.* **2006**, *47*, 7947.
[21] Boeda, F.; Crévisy, C. (Unpublished results).
[22] Wang, D.-Y.; Hu, X.-P.; Huang, J.-D.; Deng, J.; Yu, S.-B.; Duan, Z.-C.; Xu, X.-F.; Zheng, Z. *Angew. Chem. Int. Ed.* **2007**, *46*, 7810.
[23] Boeda, F.; Rix, D.; Clavier, H.; Crévisy, C. ; Mauduit, M. *Tetrahedron: Asymmetry* **2006**, *17*, 2726.
[24] (a) Zhang, W.; Zhang, X. *J. Org. Chem.* **2007**, *72*, 1020. (b) Zhang, W.; Zhang, X. *Angew. Chem. Int. Ed.* **2006**, *45*, 5515.
[25] Wehman, P.; van Donge, H. M. A.; Hagos, A.; Kamer, P. C. J.; van Leeuwen, P. W. N. M. *J. Organomet. Chem.* **1997**, *535*, 183.
[26] For classical conditions used in the synthesis of phosphoramidite group, see: References [4a, 5b] and (a) Alexakis, A.; Burton, J.; Vastra, J.; Benhaim, C.; Fournioux X.; van de Heuvel, A.; Levêque, J. M.; Mazé, F; Rosset, S. *Eur. J. Org. Chem.* **2000**, 4011. (b) Hulst, R.; de Vries, N. K.; Feringa, B. L. *Tetrahedron: Asymmetry* **1994**, *5*, 699.
[27] (a) Tu, T.; Zhou, Y.-G.; Hou, X.-L.; Dai, L.-X.; Dong, X.-C.; Yu, Y.-H.; Sun, J. *Organometallics* **2003**, *22*, 1255. (b) Boaz, N. W.; Debenham, S. D.; Mackenzie, E. B.; Large, S. E. *Org. Lett.* **2002**, *4*, 2421.
[28] van Oort, A. B.; Budzelaar, P. H. M.; Frijns, J. H. G.; Orpen, A. G. *J. Organomet. Chem.* **1990**, *396*, 33.
[29] Lot, O.; Suisse, I.; Mortreux, A.; Agbossou, F. *J. Mol. Catal. A.* **2000**, *164*, 125.
[30] Naily, S.; Suisse, I.; Mortreux, A.; Agbossou-Niedercorn, F.; Nowogrocki, G. *J. Organomet. Chem.* **2001**, *628*, 114.
[31] Cesarotti, E.; Araneo, S.; Rimoldi, I.; Tassi, S. *J. Mol. Catal. A.* **2003**, *204-205*, 211.
[32] Diéguez, M.; Ruiz, A.; Claver, C. *Tetrahedron: Asymmetry* **2001**, *12*, 2827.
[33] Diéguez, M.; Ruiz, A.; Claver, C. *Tetrahedron: Asymmetry* **2001**, *12*, 2861.
[34] Diéguez, M.; Ruiz, A.; Claver, C. *Chem. Commun.* **2001**, 2702.
[35] Raluy, E.; Claver, C.; Pamies, O.; Diéguez, M. *Org. Lett.* **2007**, *9*, 49.
[36] Mata, Y.; Claver, C.; Diéguez, M.; Pamies, O. *Tetrahedron: Asymmetry* **2006**, *17*, 3282.
[37] Mata, Y.; Diéguez, M.; Pamies, O.; Biswas, K.; Woodward, S. *Tetrahedron: Asymmetry* **2007**, *18*, 1613.
[38] Cramer, N.; Laschat, S.; Baro, A. *Organometallics* **2006**, *25*, 2284.
[39] Fraser, P. K.; Woodward, S. *Chem. Eur. J.* **2003**, *9*, 776.
[40] Cesarotti, E.; Rimoldi, I. *Tetrahedron: Asymmetry* **2004**, *15*, 3841.
[41] Arena, C. G.; Drommi, D.; Faraone, F. *Tetrahedron: Asymmetry* **2000**, *11*, 4753.
[42] Doherty, S.; Robins, E. G.; Pal, I.; Newman, C. R.; Hardacre, C.; Rooney, D.; Mooney, D. A. *Tetrahedron: Asymmetry* **2003**, *14*, 1517.
[43] (a) Hodgson, R.; Douthwaite, R. E. *J. Organomet. Chem.* **2005**, *690*, 5822. (b) Bonnet, L. G.; Douthwaite, R. E.; Kariuki, B. M. *Organometallics* **2003**, *22*, 4187.
[44] Bronger, R. P. J.; Guiry, P. J. *Tetrahedron: Asymmetry* **2007**, *18*, 1094.

Received: October 31, 2007 **Revised: March 04, 2008** **Accepted: March 08, 2008**